



**The Abdus Salam  
International Centre for Theoretical Physics**



**2137-30**

**Joint ICTP-IAEA Advanced Workshop on Multi-Scale Modelling for  
Characterization and Basic Understanding of Radiation Damage  
Mechanisms in Materials**

*12 - 23 April 2010*

**The experimental validation of radiation damage modeling**

M. Victoria

*Nuclear Fusion Institute, Universidad Politecnica de Madrid  
Spain*

Joint ICTP-IAEA Advanced Workshop on Multi-Scale Modeling for  
Characterization and Basic Understanding of Radiation Damage  
Mechanisms in Materials, April 12-23, 2010

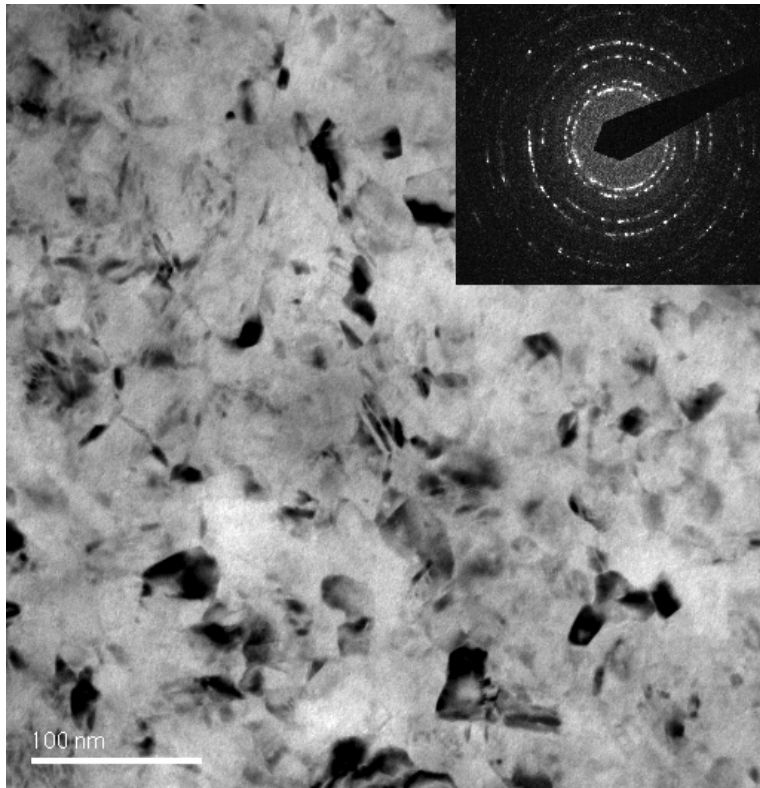


# The experimental validation of radiation damage modeling

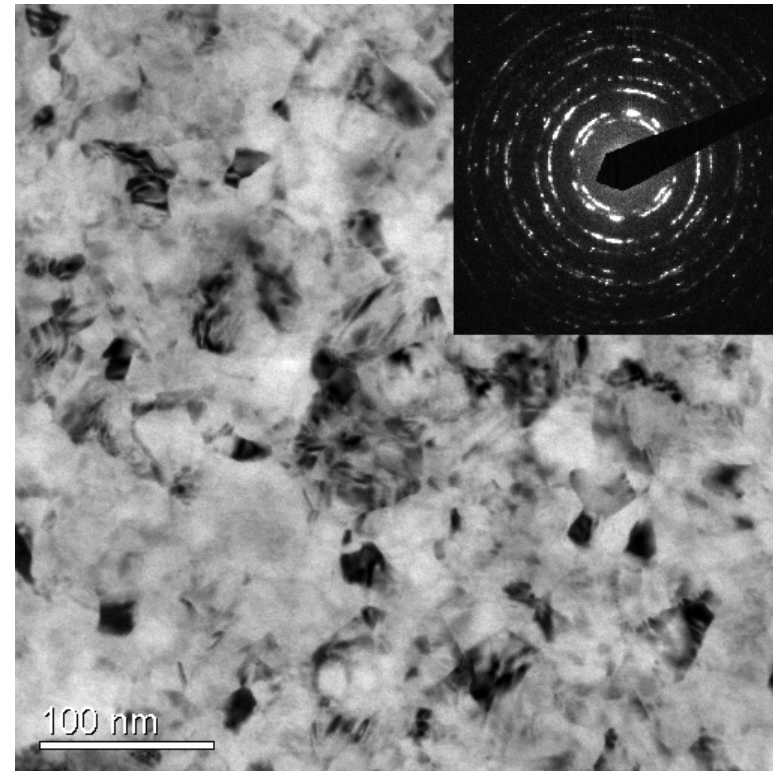
## II. The initial attempts to multiscale

Max Victoria  
Visiting Professor, UPM

# Electron microscopy: ED nc Ni

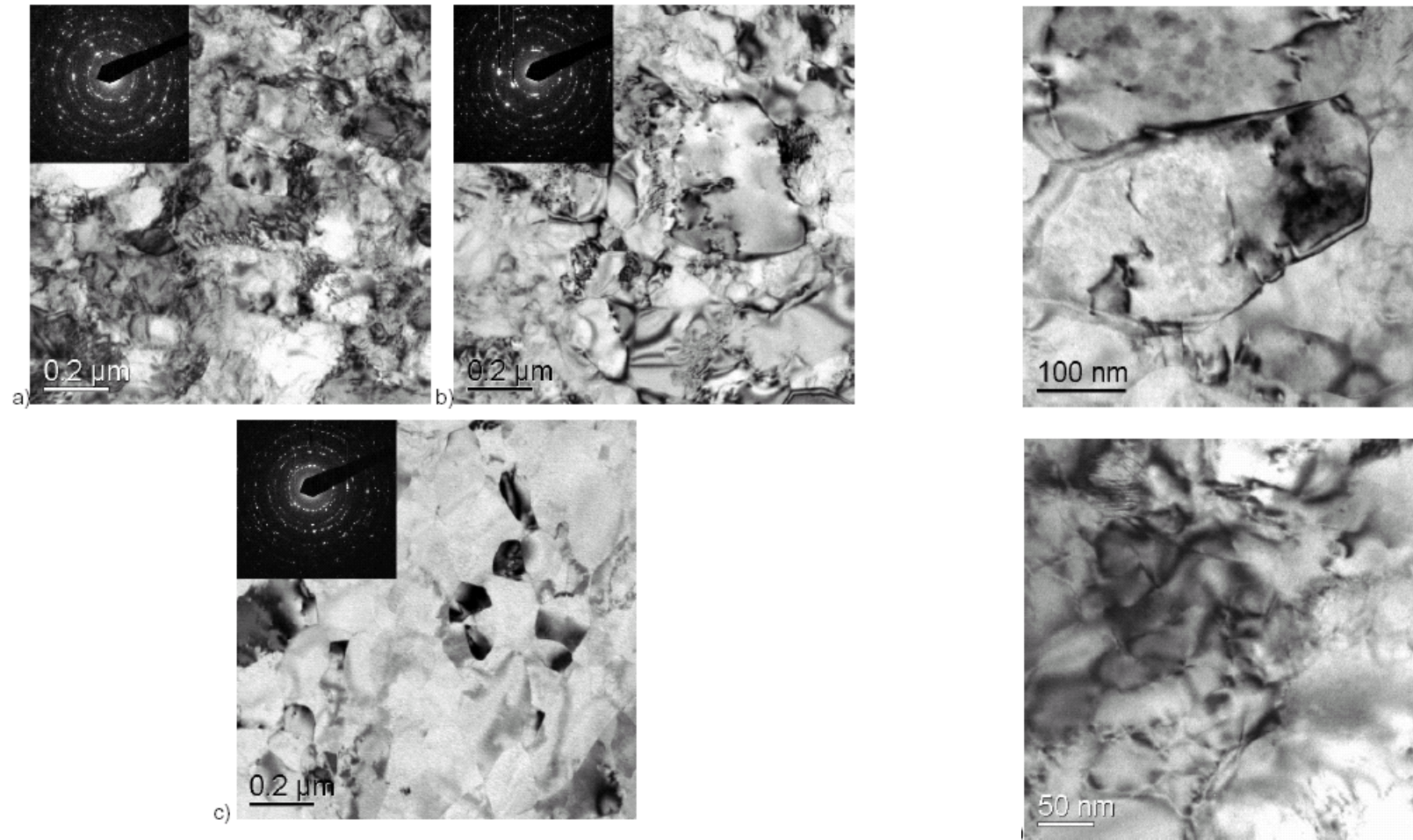


**Sample A,  $\langle 111 \rangle$ , 21.3nm**



**Sample B,  $\langle 200 \rangle$ , 20.4 nm**

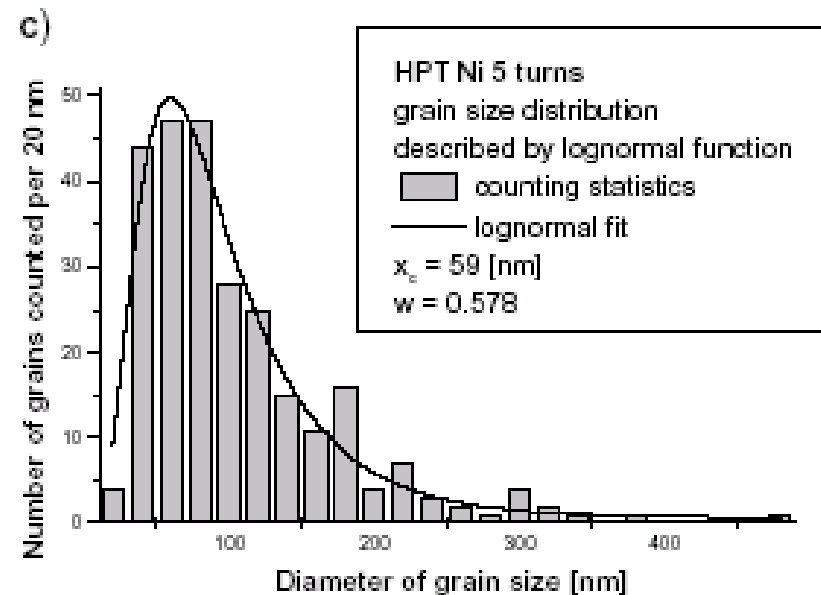
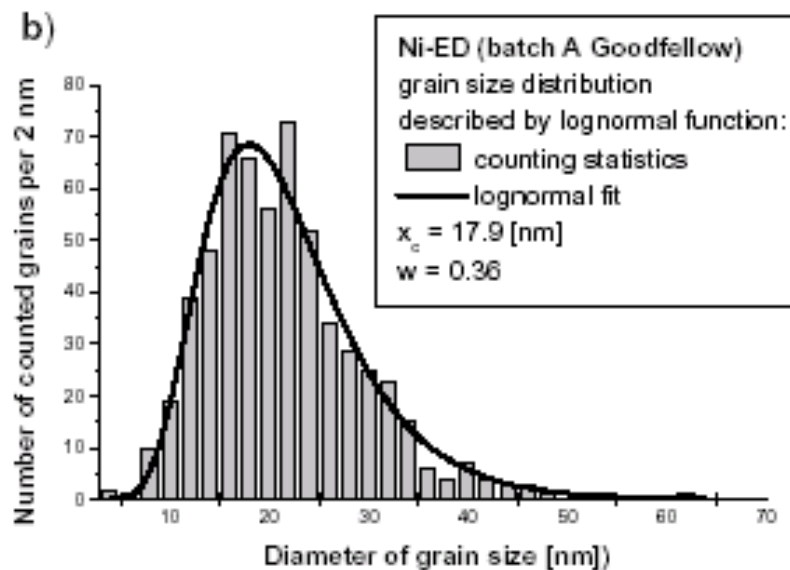
# Electron microscopy:HPT nc Ni



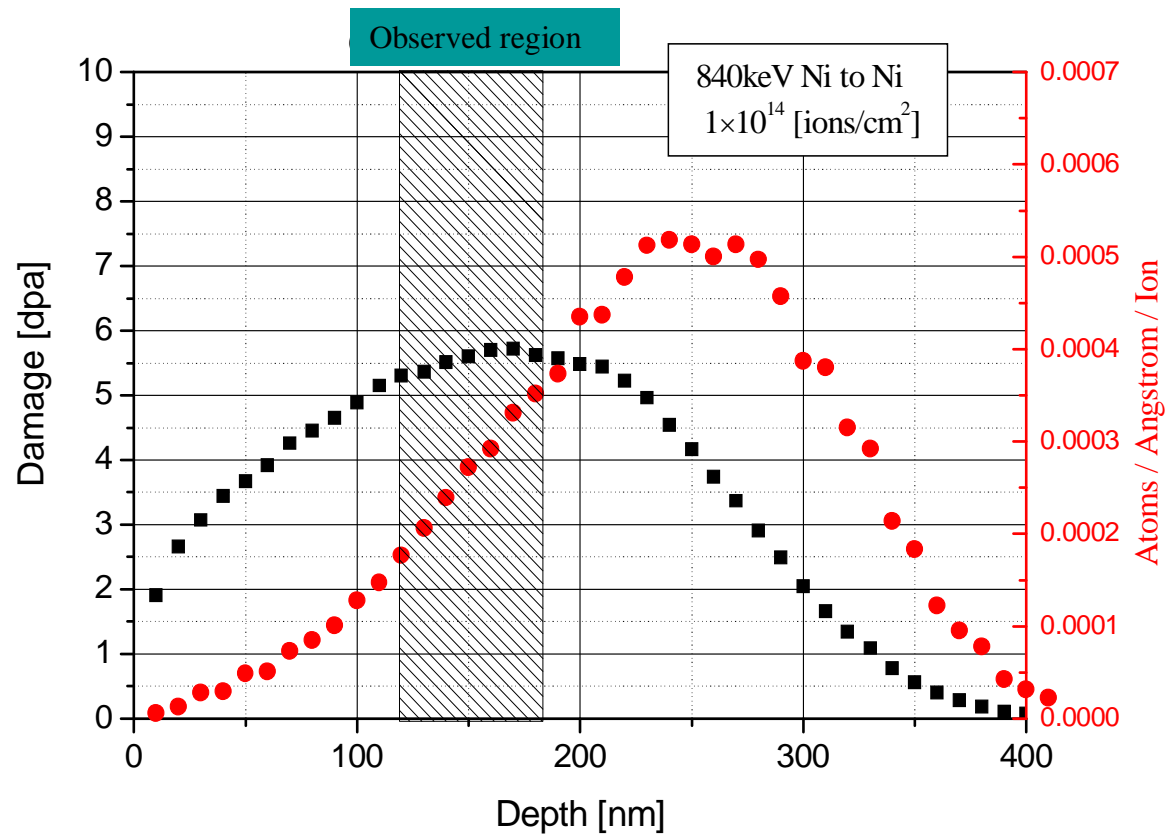
Microstructure of HPT nc Ni: a) → c)  
change in microstrains with the  
thickness of the specimen

Dislocations and subgrains  
in HPT nc Ni

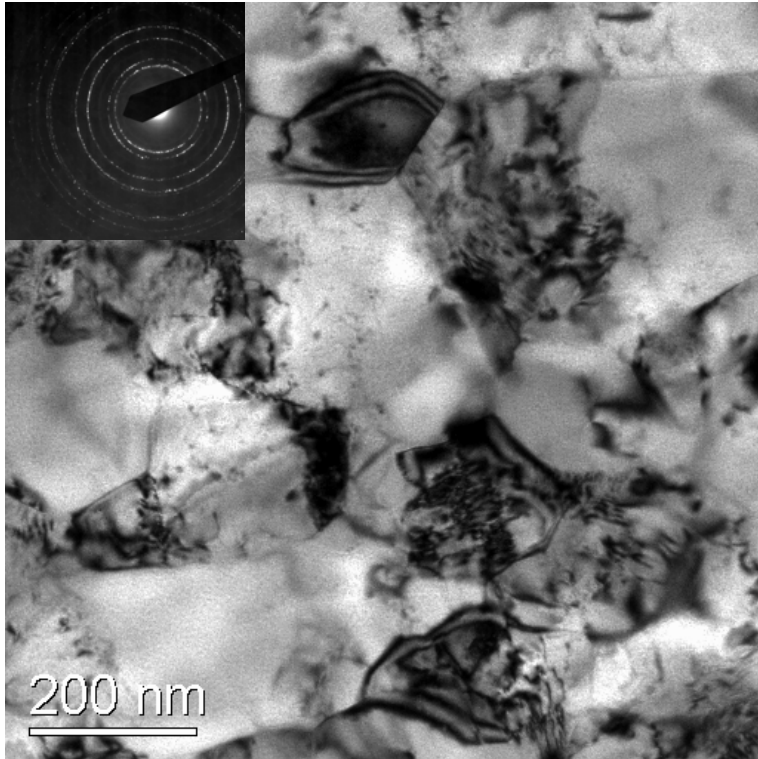
# Two synthesis methods produce different grain size distributions



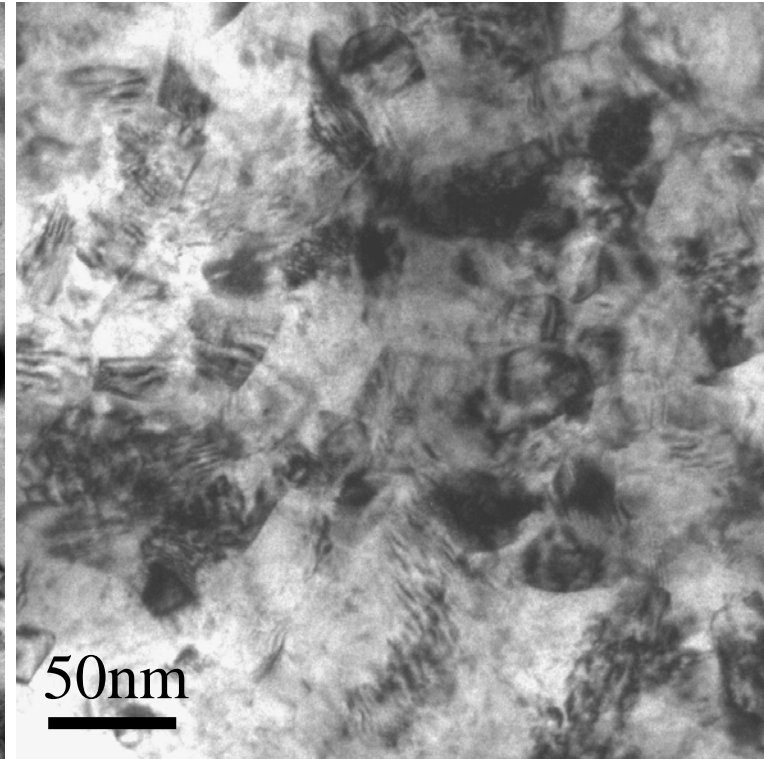
# Ni<sup>+</sup> ion irradiation conditions (TRIM)



# The microstructure of HPT Ni

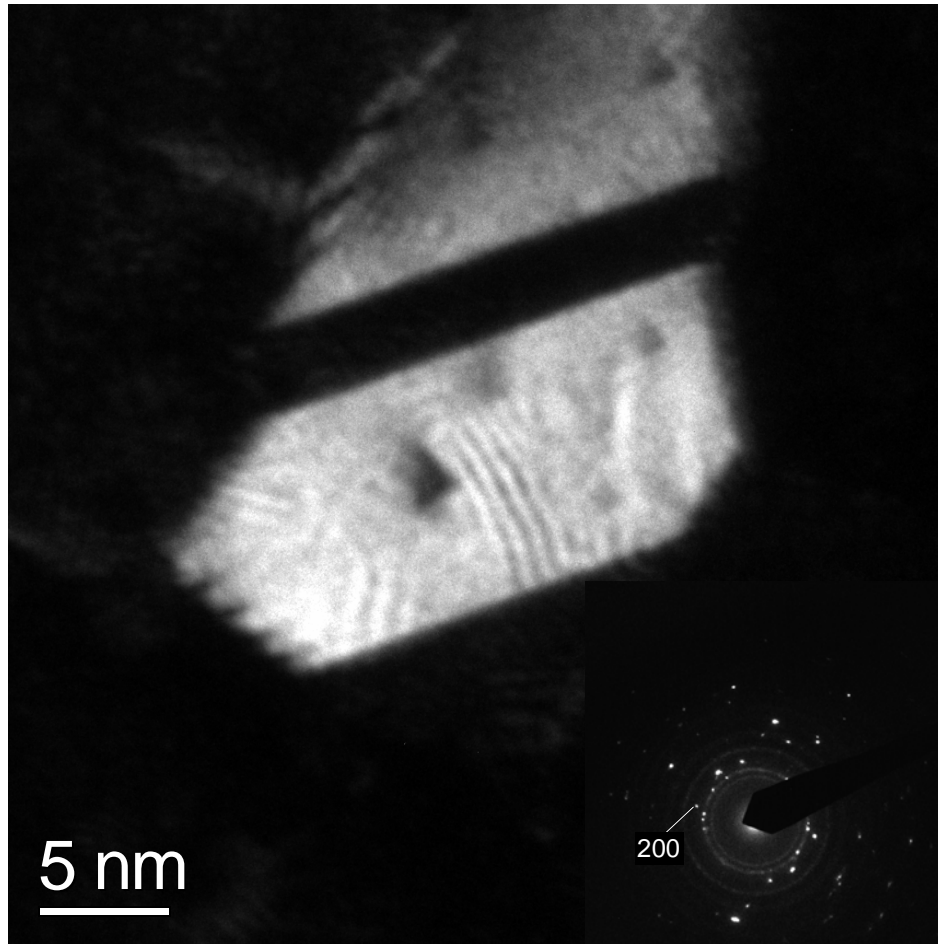


**unirradiated**



**irradiated, 0.5 dpa p<sup>+</sup>**

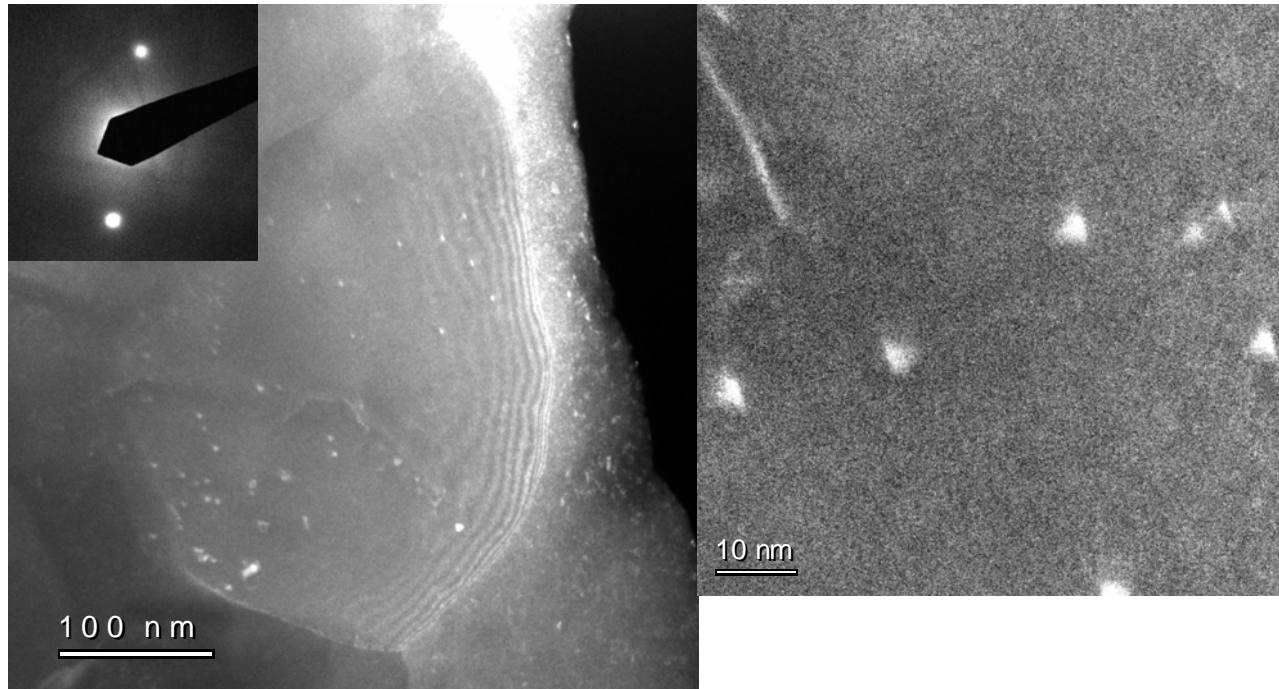
# Microstructure ED nc Ni



irradiated with  
Ni<sup>+</sup> ions to 5 dpa  
SFT density  
 $5.9 \times 10^{22} \text{ m}^{-3}$

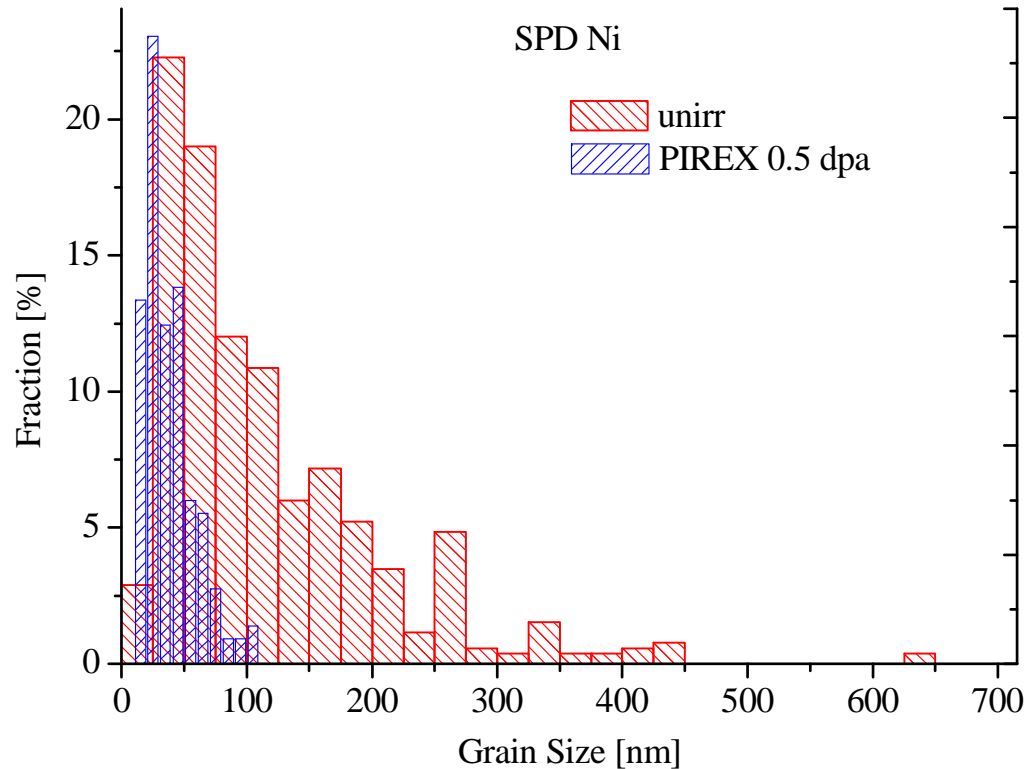
$B = \langle 110 \rangle$  and  $g = \langle 002 \rangle$ .

# Microstructure of irradiated HPT Ni



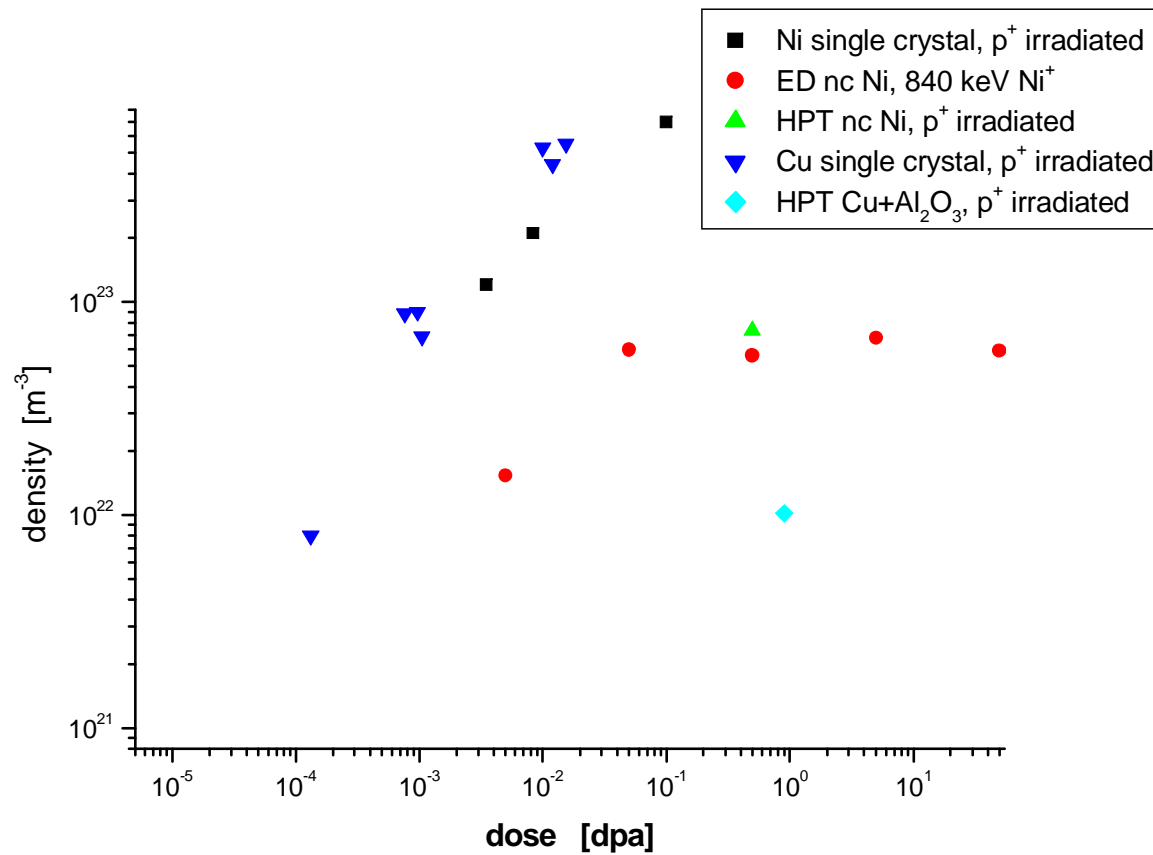
**$B = \langle 110 \rangle$  and  $g = \{002\}$ . SFT mean size: 2.5 nm, density  $7.4 \times 10^{22} \text{ m}^{-3}$**

# Grain size distribution of both unirradiated and irradiated HPT Ni

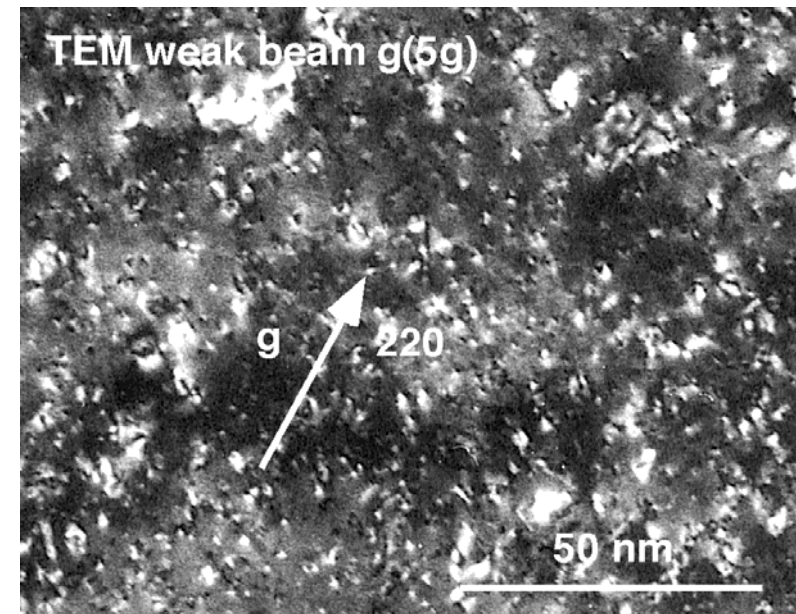
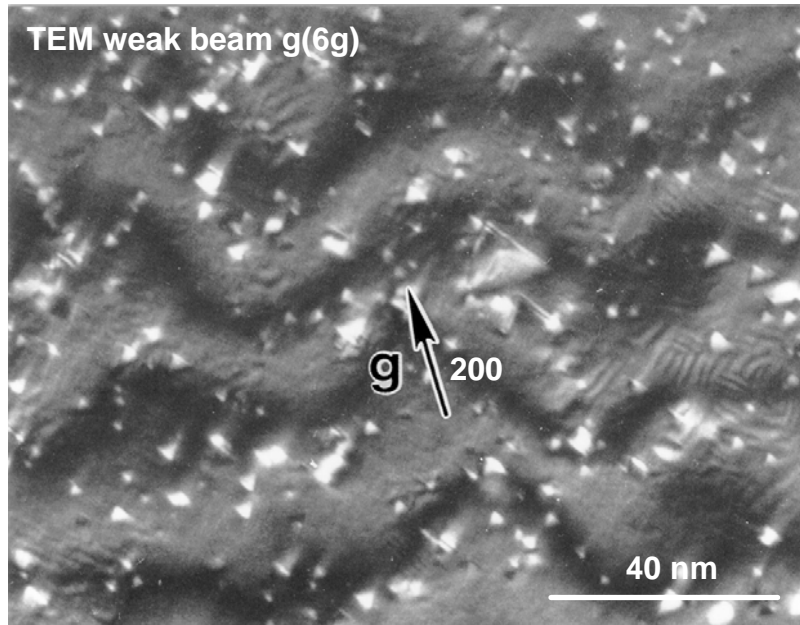


Average grain size decreases from 115 nm (unirradiated, 34 nm by XRD) to 38 nm (irradiated)

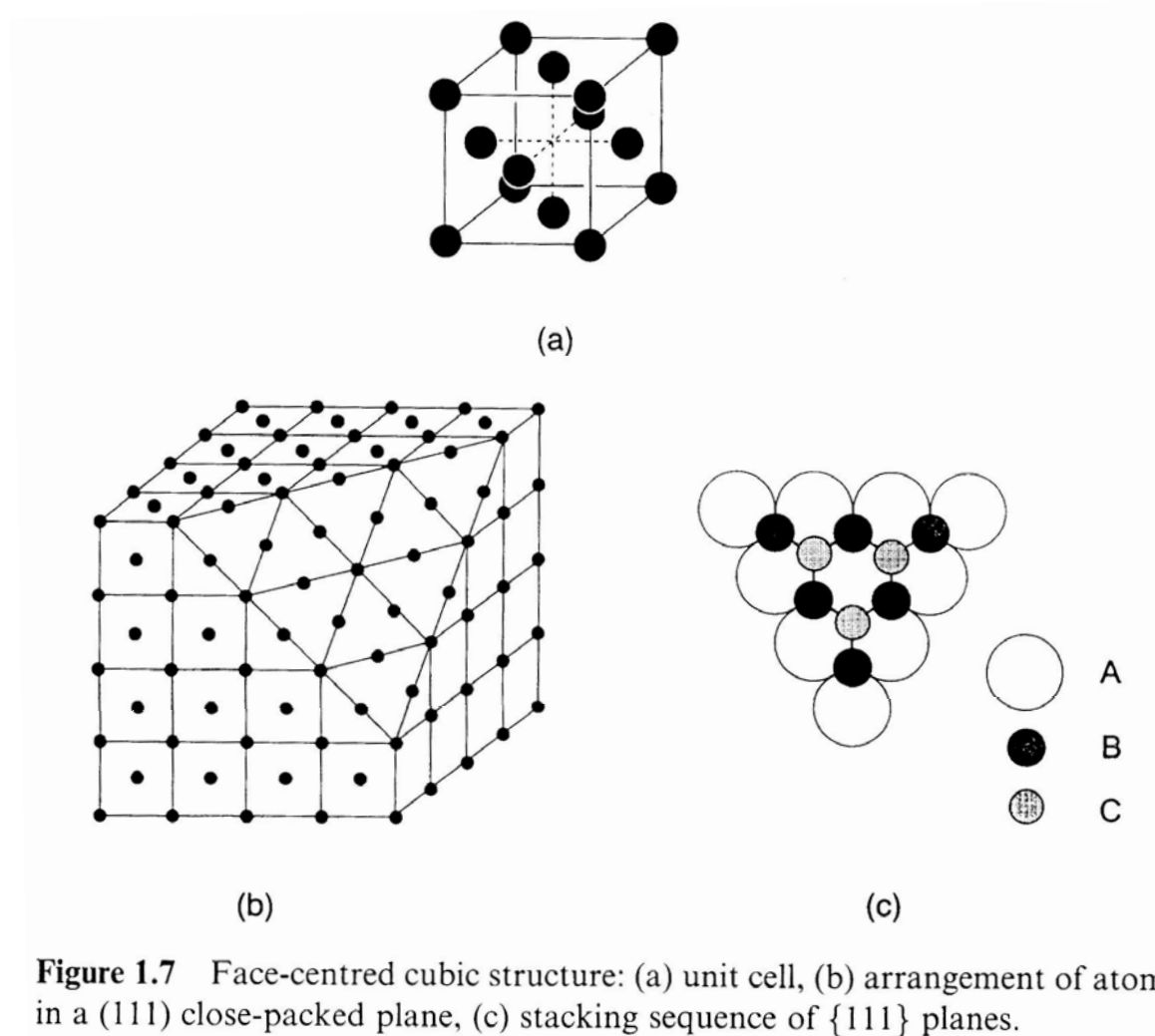
# Defect accumulation after irradiation



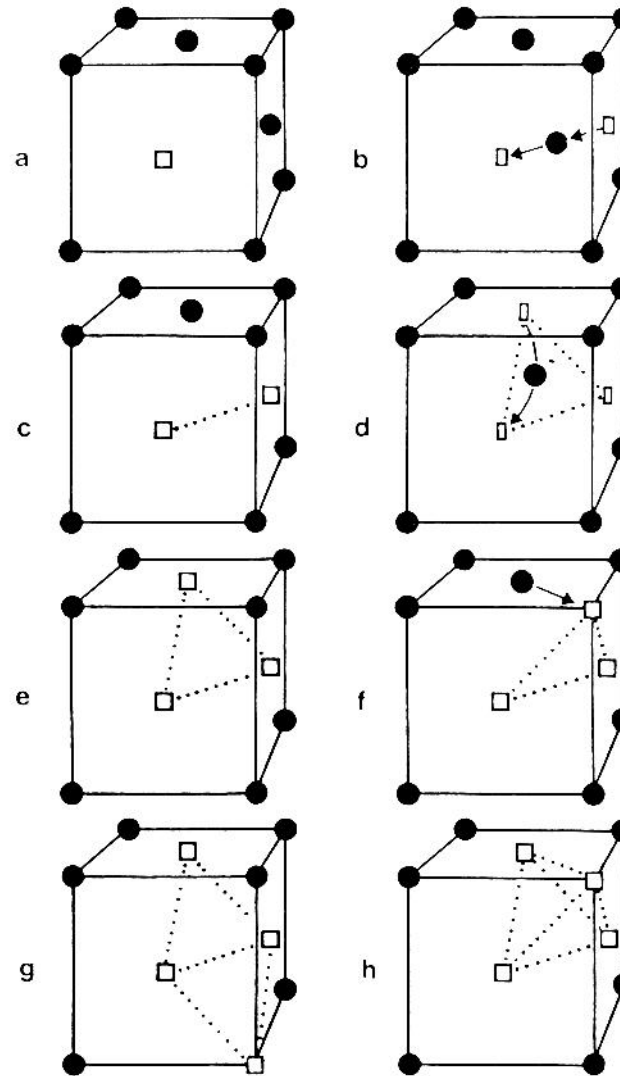
# Irradiation induced defect clusters in Cu ( $4.6 \cdot 10^{-2}$ dpa) and Pd ( $6.6 \cdot 10^{-2}$ dpa)



# The fcc structure

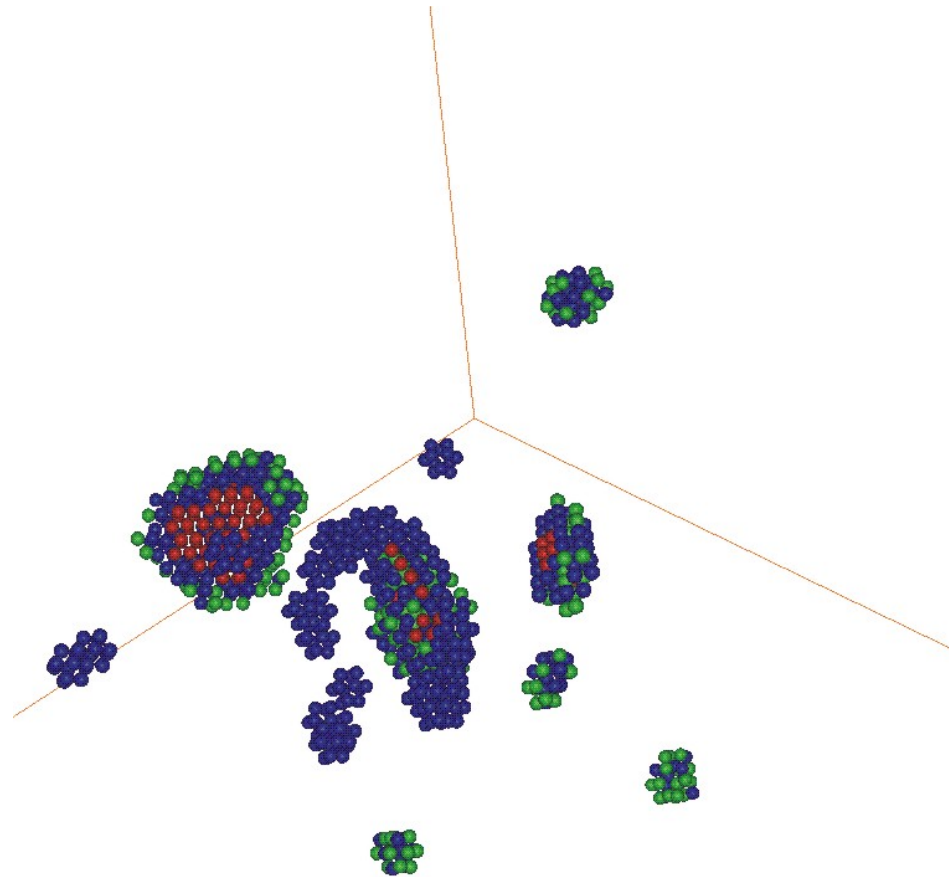


# Vacancy configurations in fcc



Vacancies in an fcc lattice: (a, b) single vacancy and migration saddle point, (c, d) divacancy and migration saddle point, (e, f) trivacancy and reorientation, (g, h) tetravacancies.

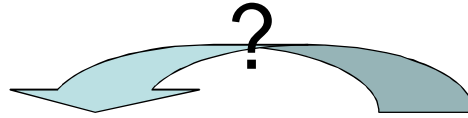
# MD simulation of 20keV PKA cascade in single crystal fcc Ni



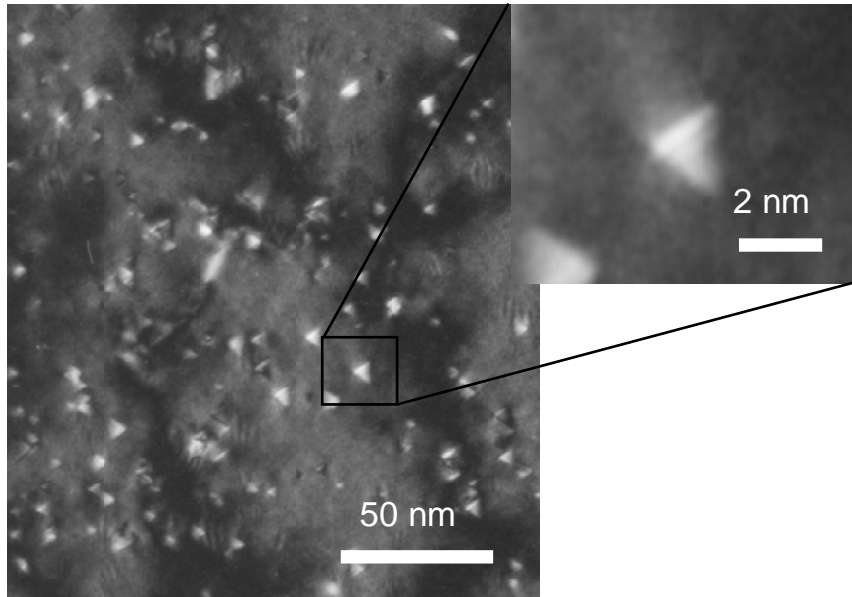
Close up of defect structure after cascade cooling.

# Visualization of the objects produced in MD simulations

e.g. Stacking fault tetrahedra in irradiated copper

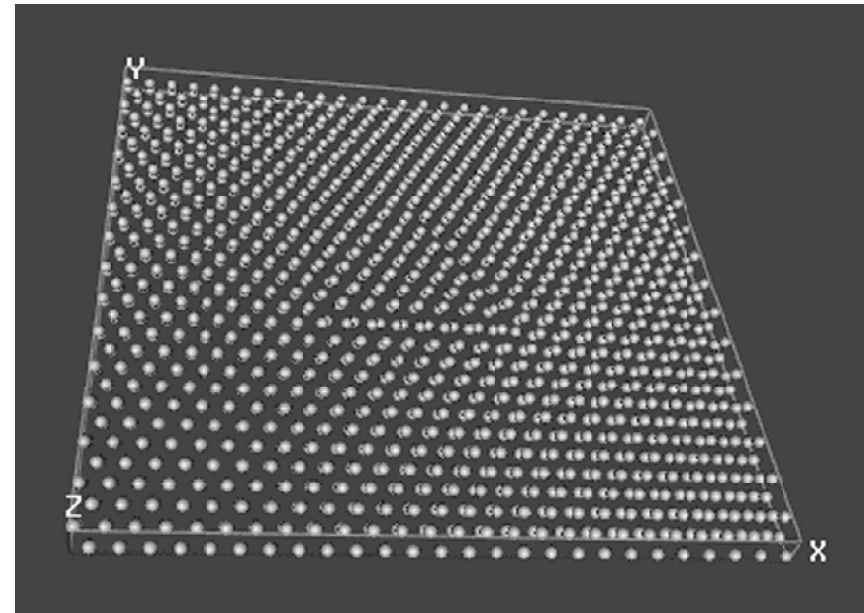


Experiments



Cu 0.01 dpa RT  
weak beam  $g(6g)$   $g = (200)$

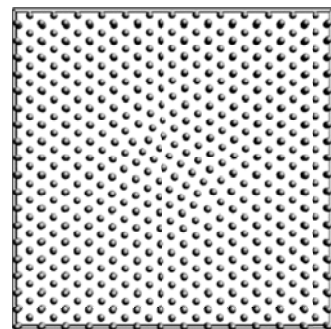
Simulations



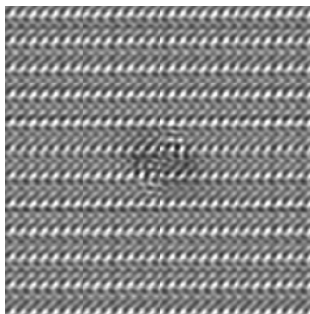
Molecular dynamics simulation  
Pair potential method, 100'000 atoms

Schaublin

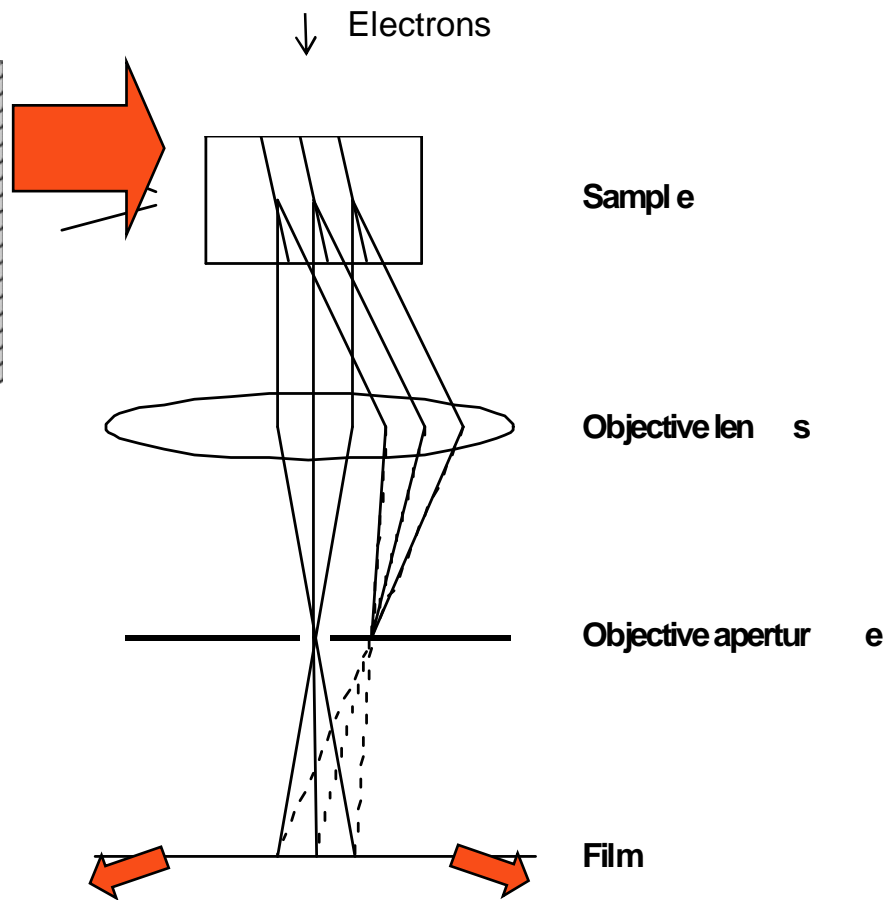
# Image formation in the electron microscope



37-interstitial Frank loop in Al



High Resolution imaging mode

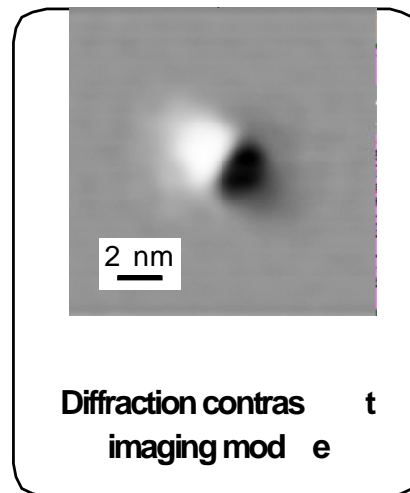


Sample

Objective lens

Objective aperture

Film



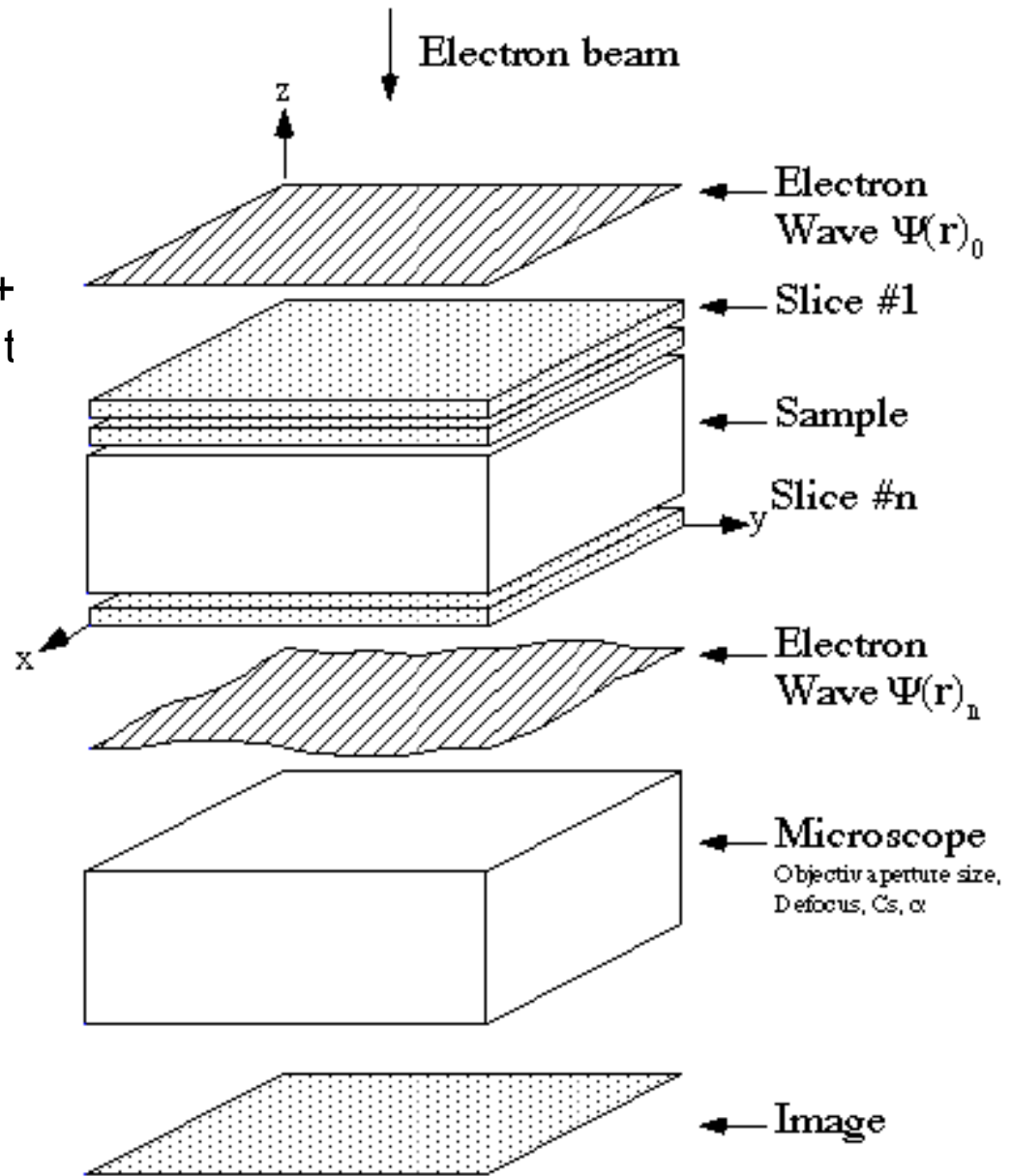
Diffraction contrast imaging mode

# Multislice technique

$$\Psi(r)_j = [\Psi(r)_{j-1} \cdot q_j] \times p_{j \rightarrow j+1}$$

$\Psi(r)_j$  : Wave function entering slice  $j$   
 $q_j$  : Function of the transmittance of slice  $j$ ,

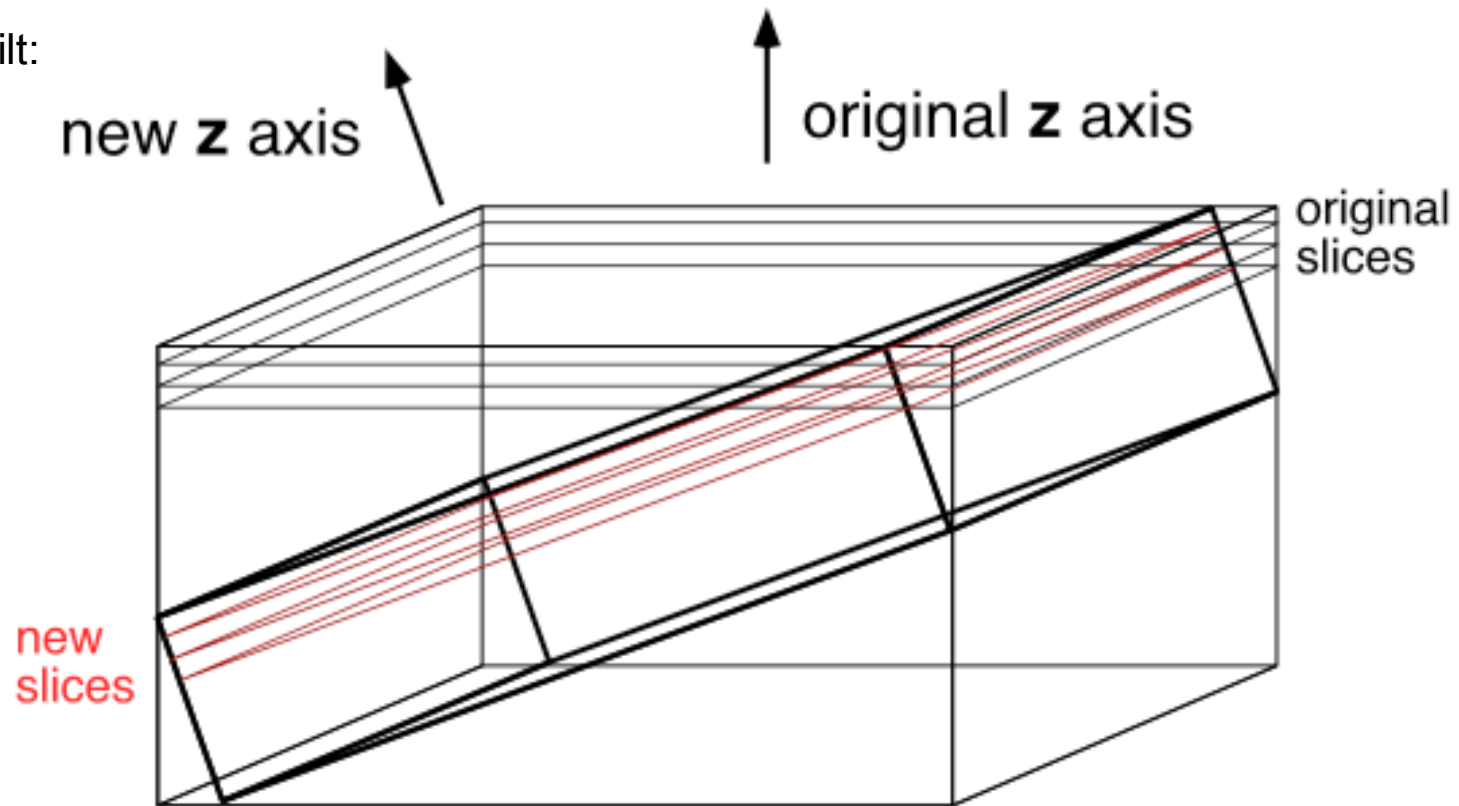
$p_{j \rightarrow j+1}$  : Function of propagation (propagator) from slice  $j$  to slice  $j+1$ .



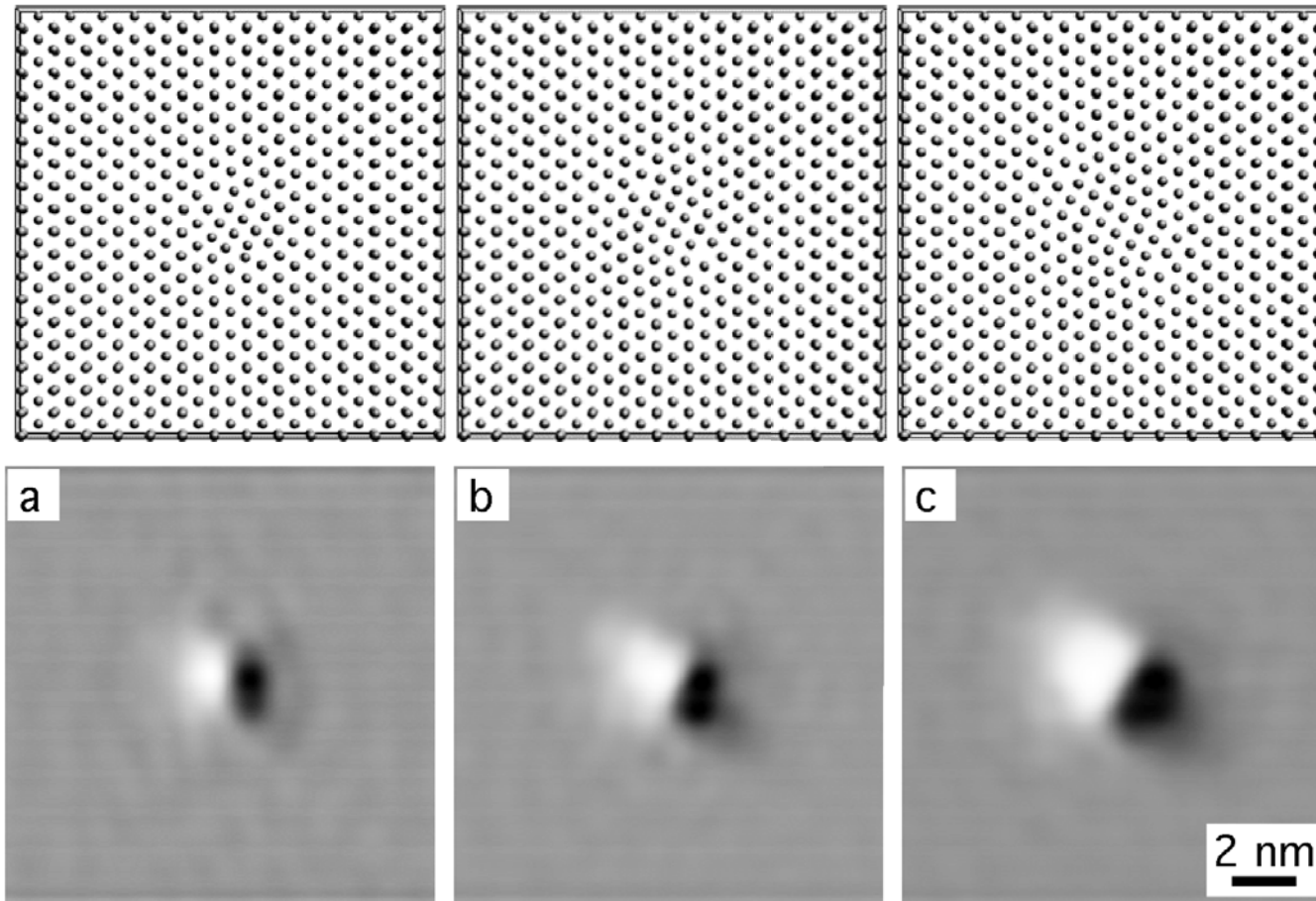
# Multislice technique

- Defining the diffraction condition

First tilt:



## The Frank loop-type cluster in Al



Interstitial Frank loop simulated TEM images using weak beam  $g(3.1g)$ ,  $g=(200)$  at 200 kV in Al for a diameter of about (a) 1.0 nm (8 interstitials), (b) 1.5 nm (19 interstitials) and (c) 2.0 nm (37 interstitials).

## Simulation of SFTs

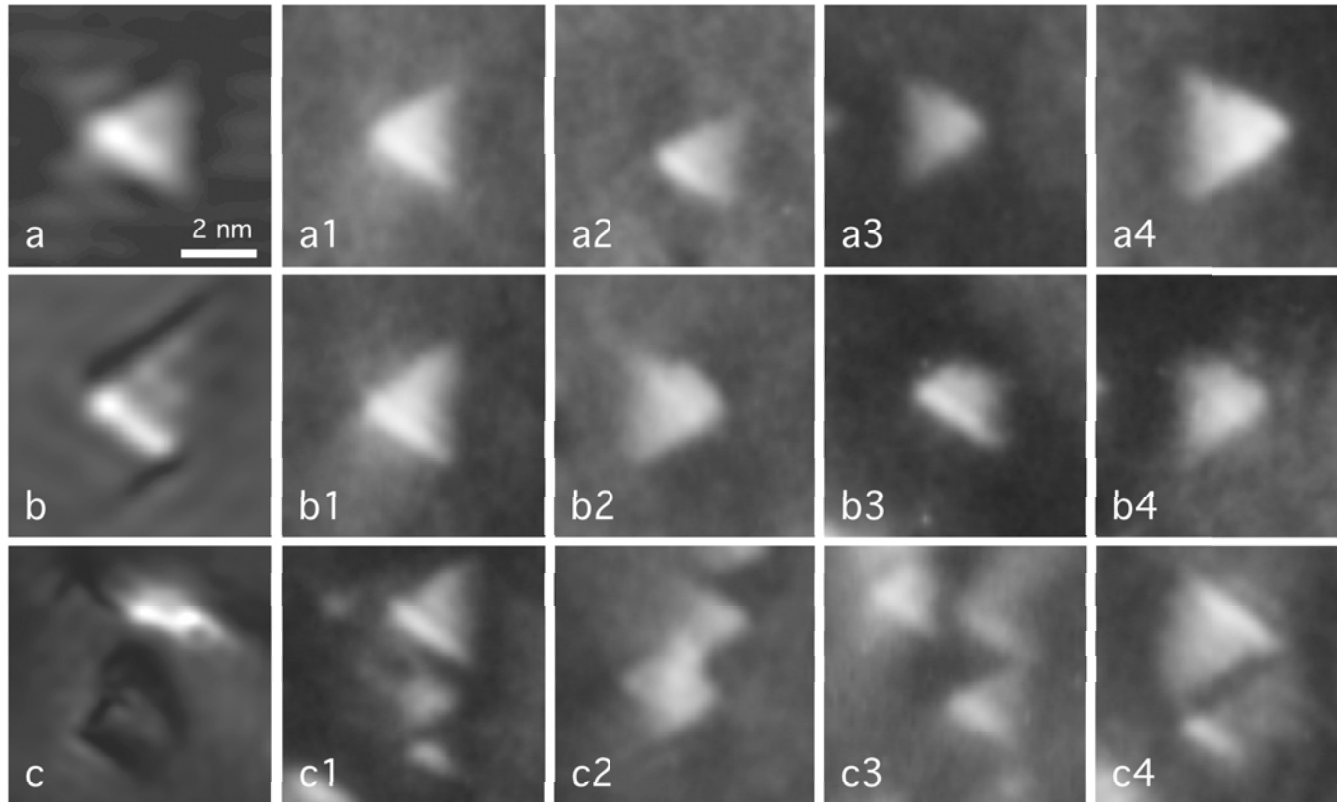
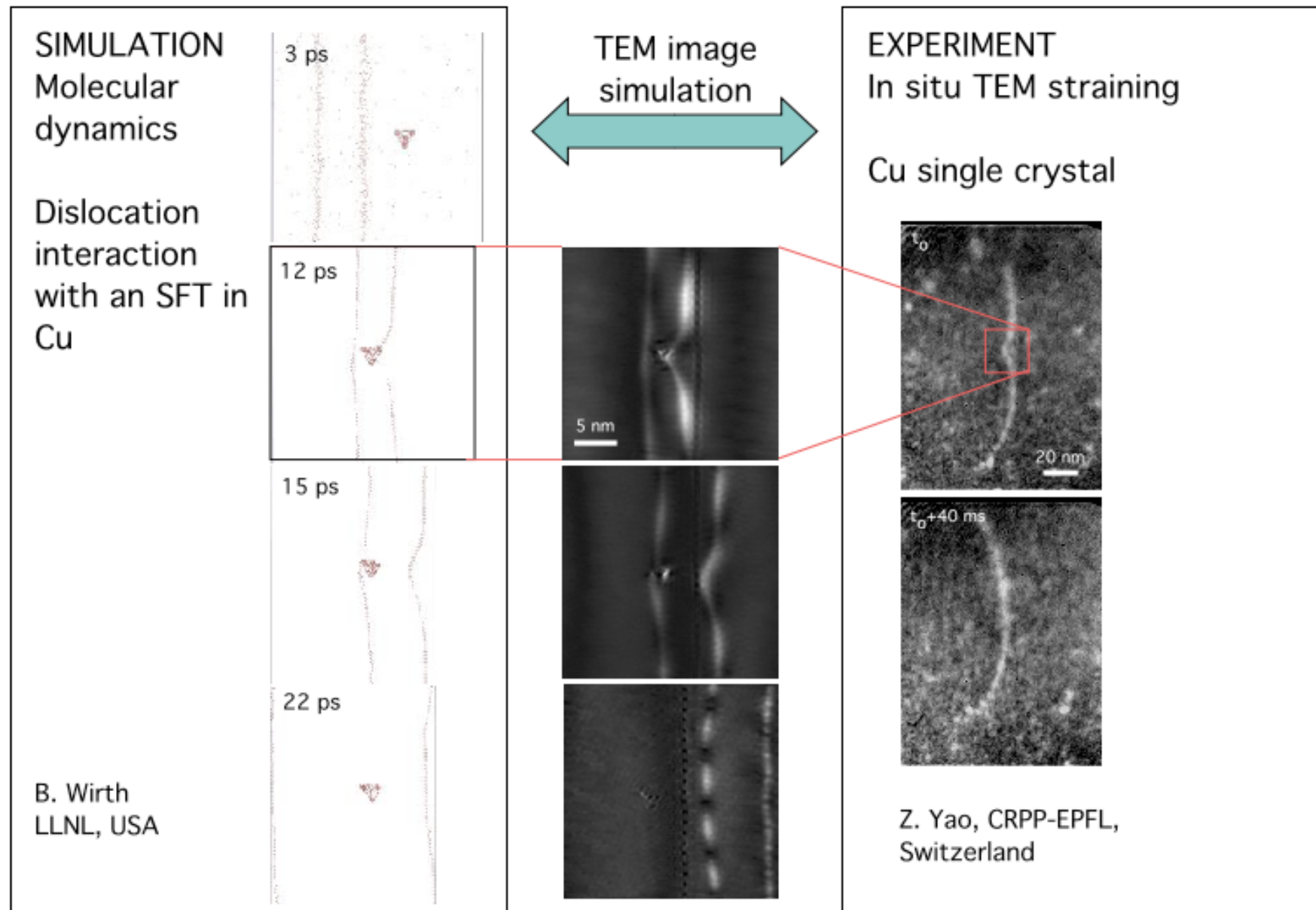


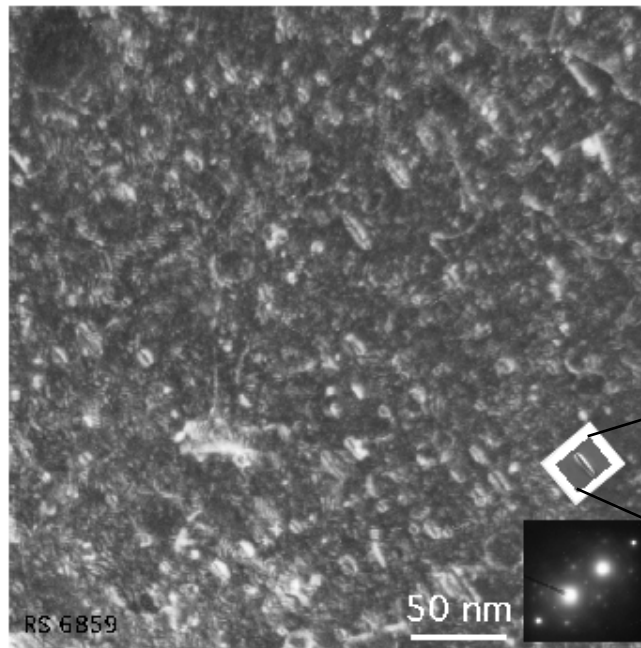
Table of TEM weak beam images in Cu irradiated at room temperature to 0.046 dpa, showing (row a) perfect SFTs, (row b) truncated SFTs and (row c) groups of intermixed SFT. First column of images (a, b and c) shows corresponding simulated images while second to fourth columns (a1-a4, b1-b4 and c1-c4) show corresponding typical experimental images of those.



# Large loops in ferritic steels

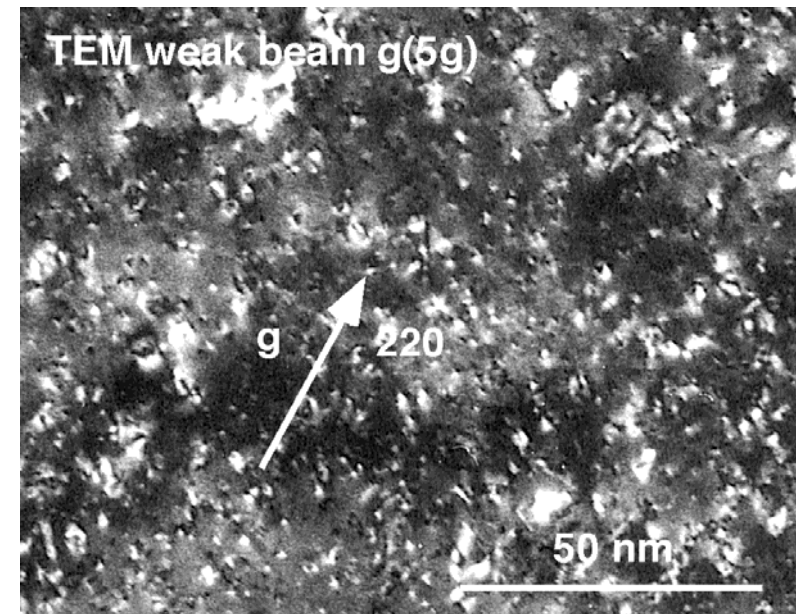
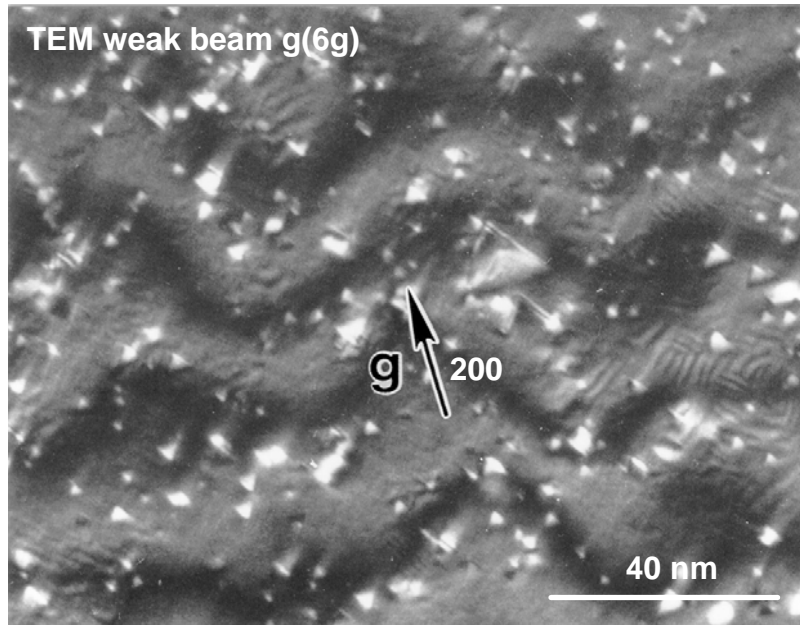
MD simulation.  
Jaime Marian LLNL USA

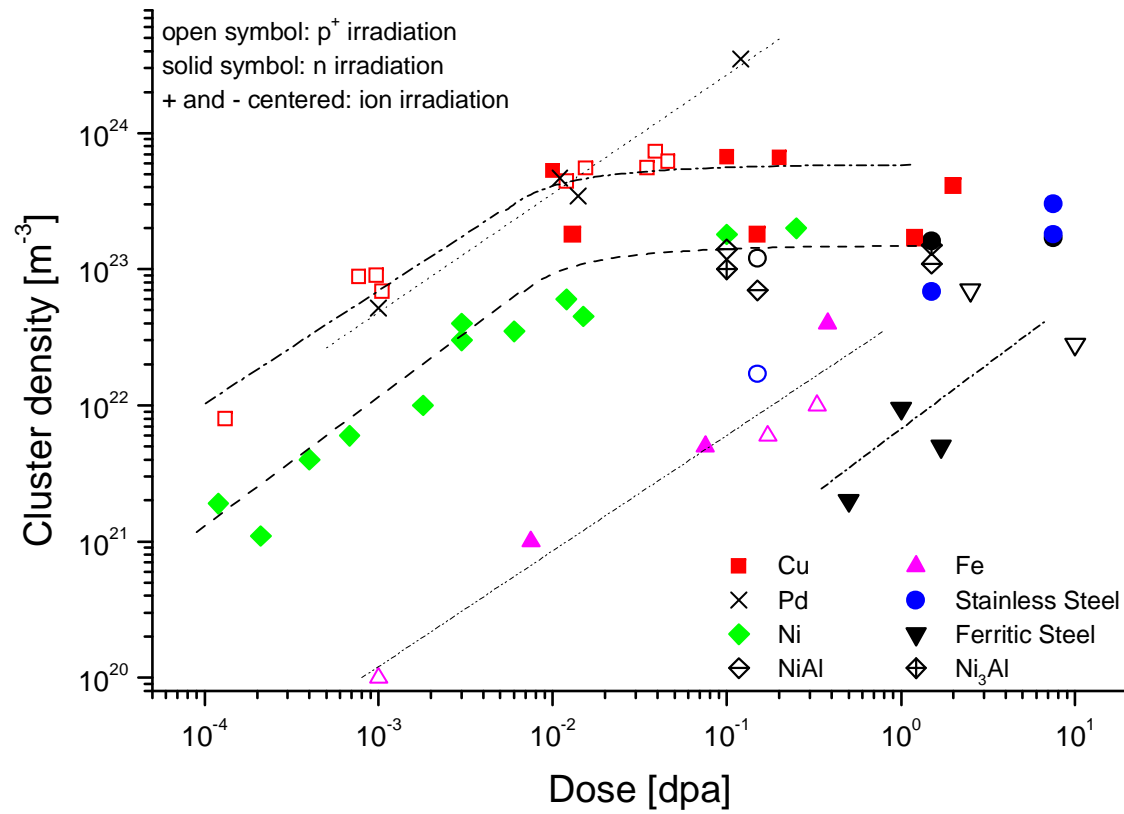
Interstitial loop in pure Fe  
937 interstitial  $\langle 100 \rangle$  loop  
on (100) plane  
Weak beam  $g(4.1g)$   $g=(200)$   
200 kV  
thickness 18 nm  
Image width = 22.9 nm



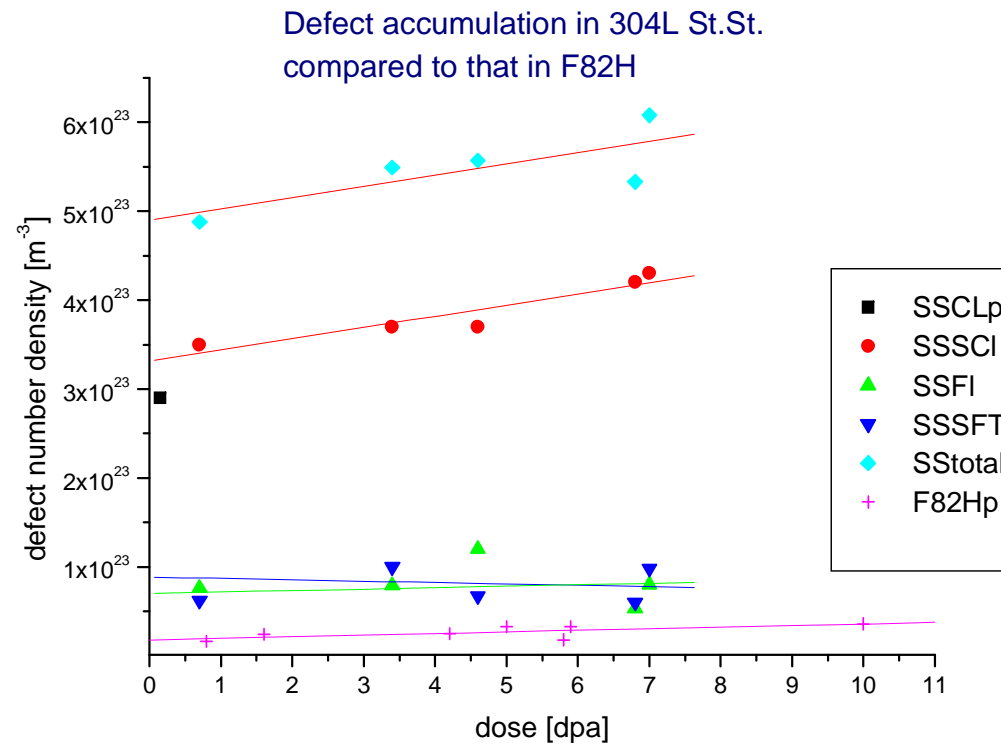
F82H, 8.8 dpa, Weak beam  $g(3.1g)$   
 $g=(200)$  200 kV thickness ~60 nm

# Irradiation induced defect clusters in Cu ( $4.6 \cdot 10^{-2}$ dpa) and Pd ( $6.6 \cdot 10^{-2}$ dpa)





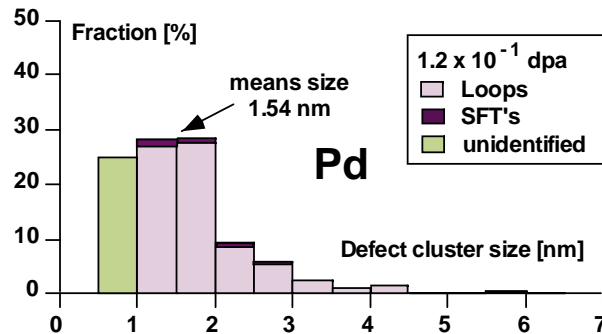
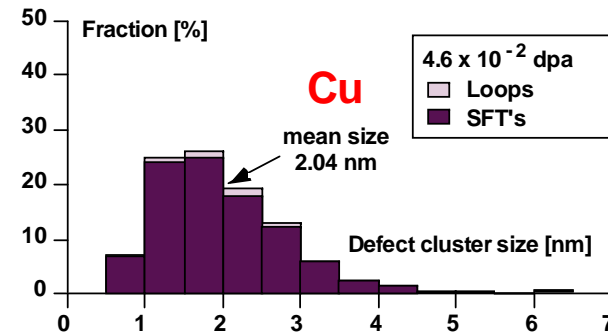
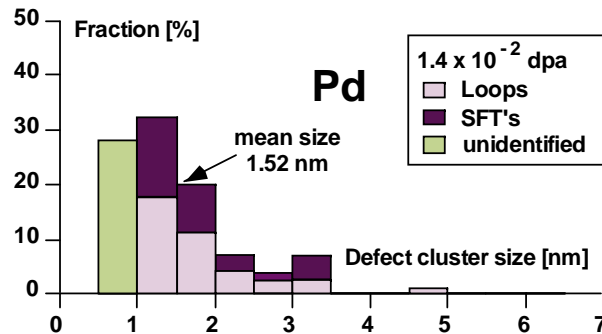
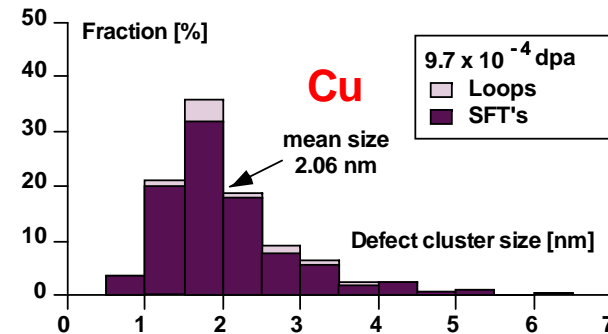
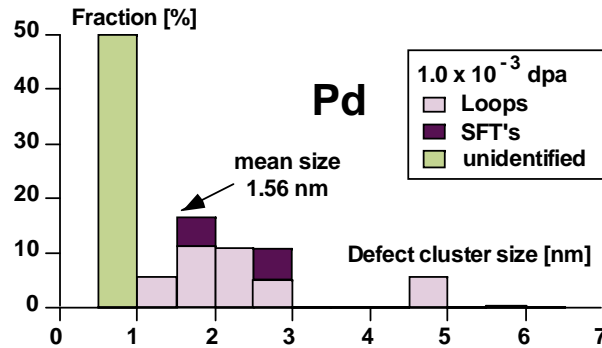
# Defect accumulation in technical alloys





# Defect cluster Size and Type

the irradiation products are mainly dislocation loops in Pd and stacking fault tetrahedra in Cu



# The cluster defect microstructure

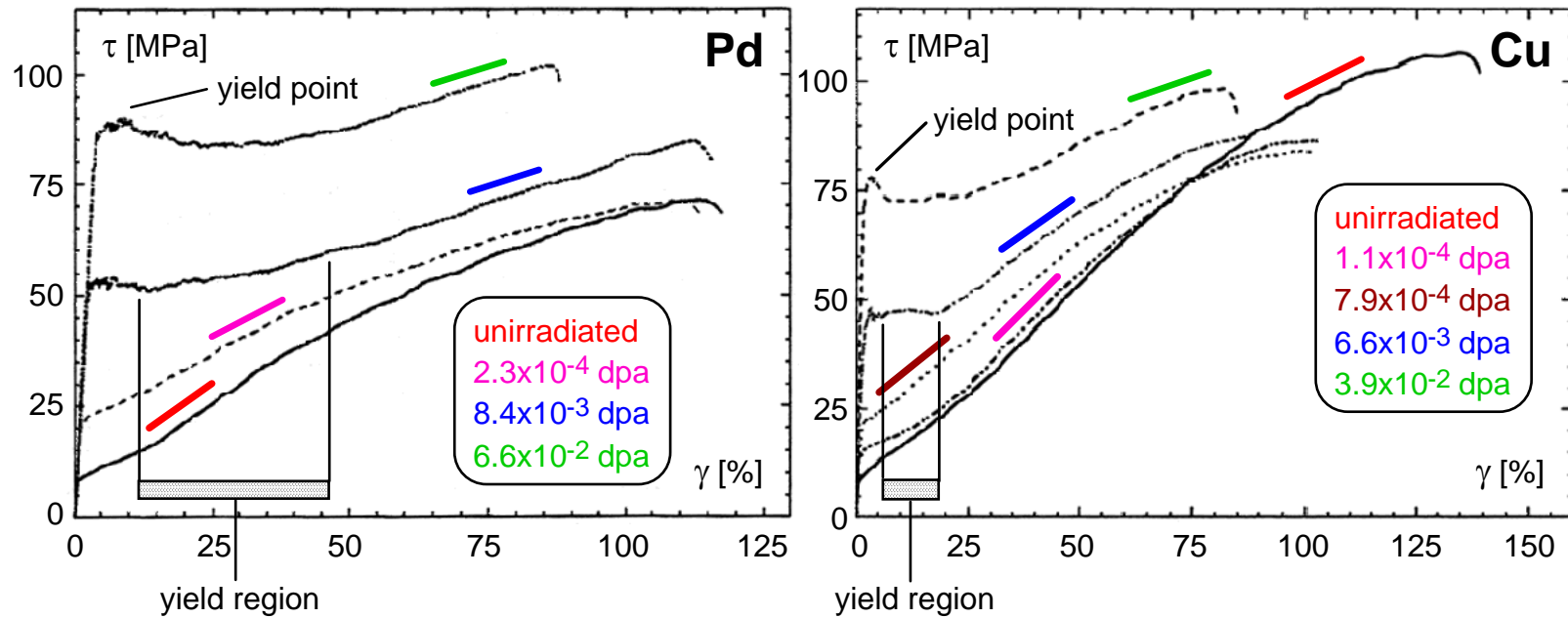
- The stacking fault energy plays a role in defining the type of defect cluster formed. In low SFE Cu ( $45 \text{ mJ m}^{-2}$ ) the majority of defects observed are SFT's. As the SFE increases, SFT are more difficult to form the tendency is to form loops as in Pd ( $180 \text{ mJ m}^{-2}$ ). But it is not the only controlling factor as indicated by the 304L st. st. ( $40 \text{ mJ.m}^{-2}$ ).
- While the mean size of SFT's remains constant with dose (low vacancy mobility), loops will grow beyond a certain dose (stainless steels) or temperature (Fe) by accumulation of mobile SIA clusters, developing a broad size distribution.

# The cluster defect microstructure

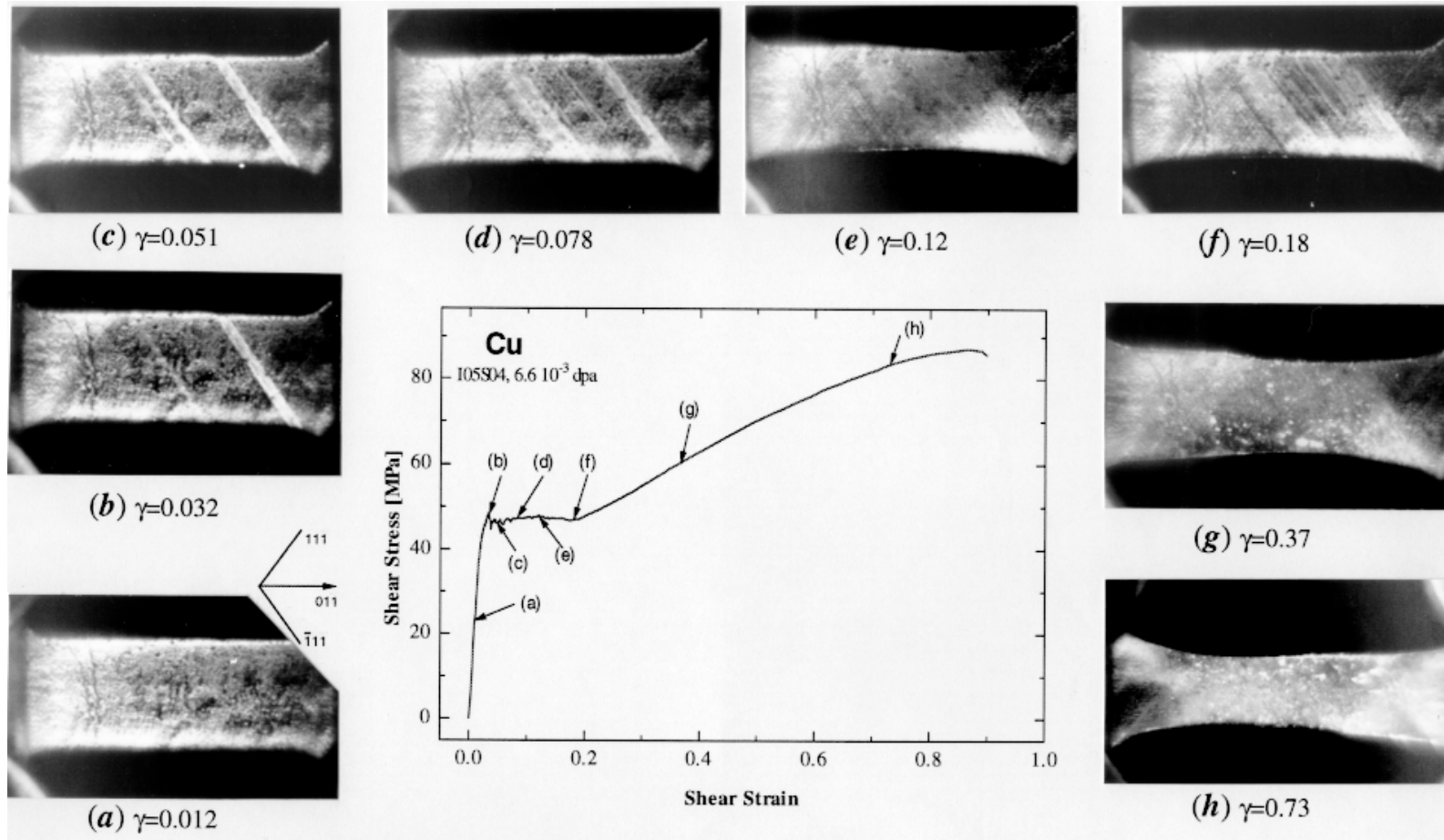
- An almost a linear dependence is found for the density of defects in Cu, Pd or Fe (slope of the log/log plot  $\sim 0.9$ ). But in Fe, three orders of magnitude higher dose are needed to attain the same defect density.
- Based in particular in the results for SFT's in Cu, the dose dependence of the number density can be taken as an indication that the majority of the defect clusters actually originate from the cascade

# Stress-Strain Curves

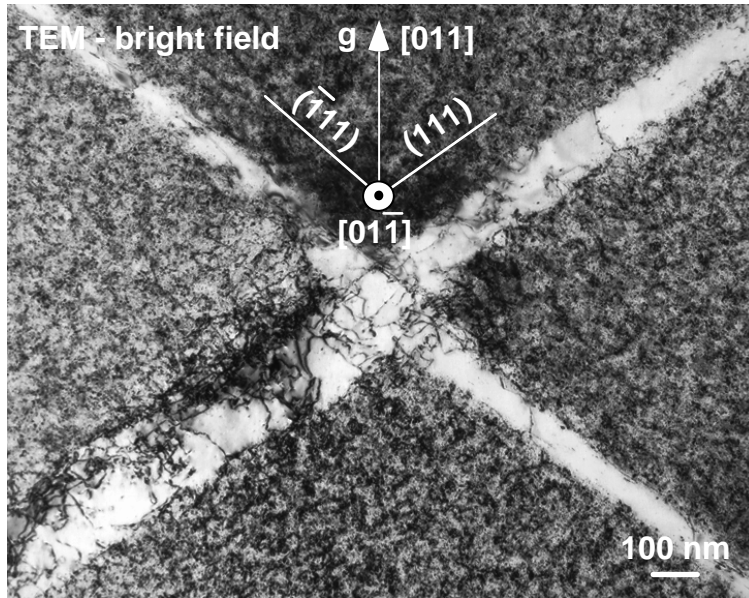
irradiation induces hardening and embrittlement  
(apparition of a yield point and a yield region)



# Localized deformation in irradiated Cu

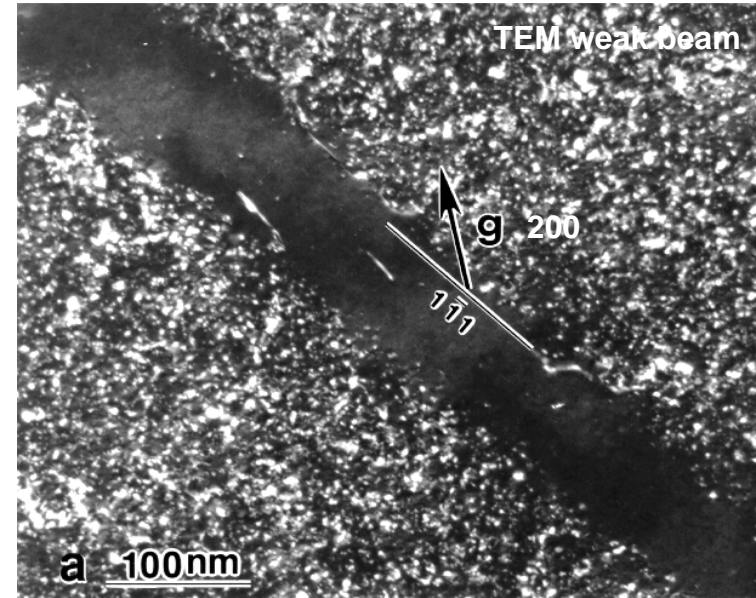


# Defect-Free Channels



## Palladium

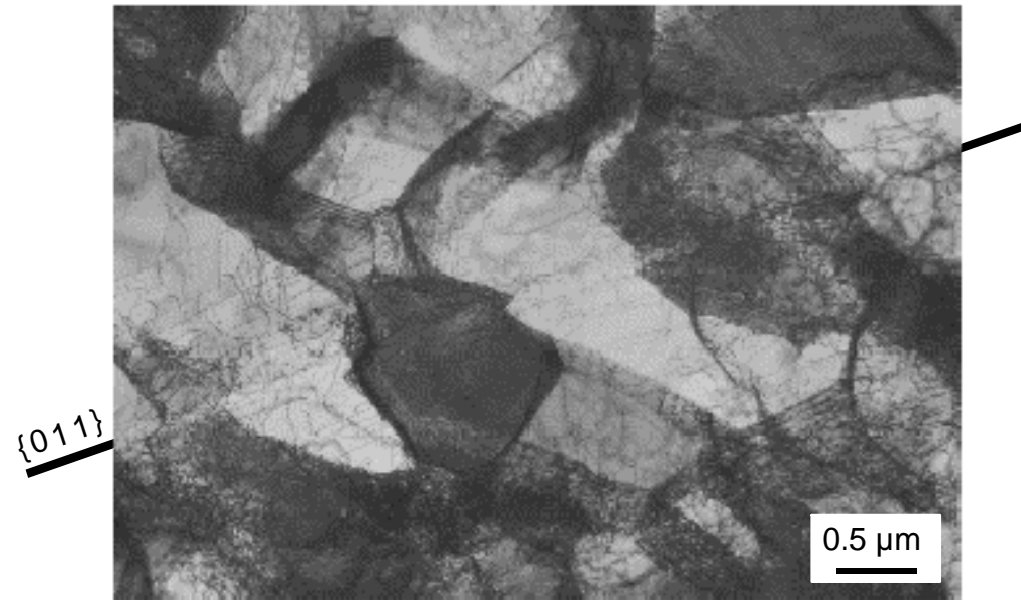
$6.6 \times 10^{-2}$  dpa  
 $\gamma = 80 \%$



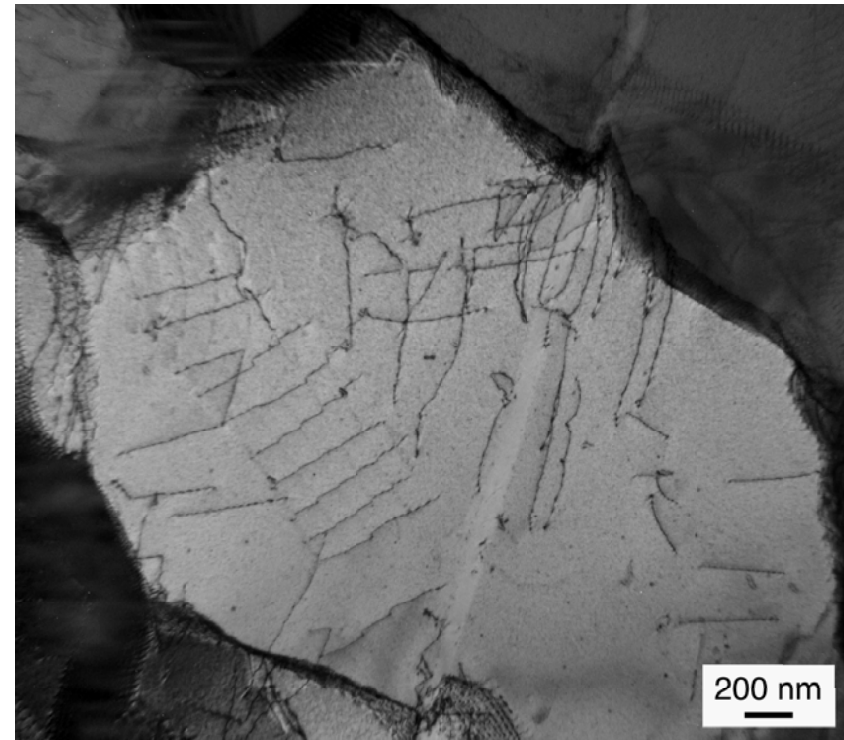
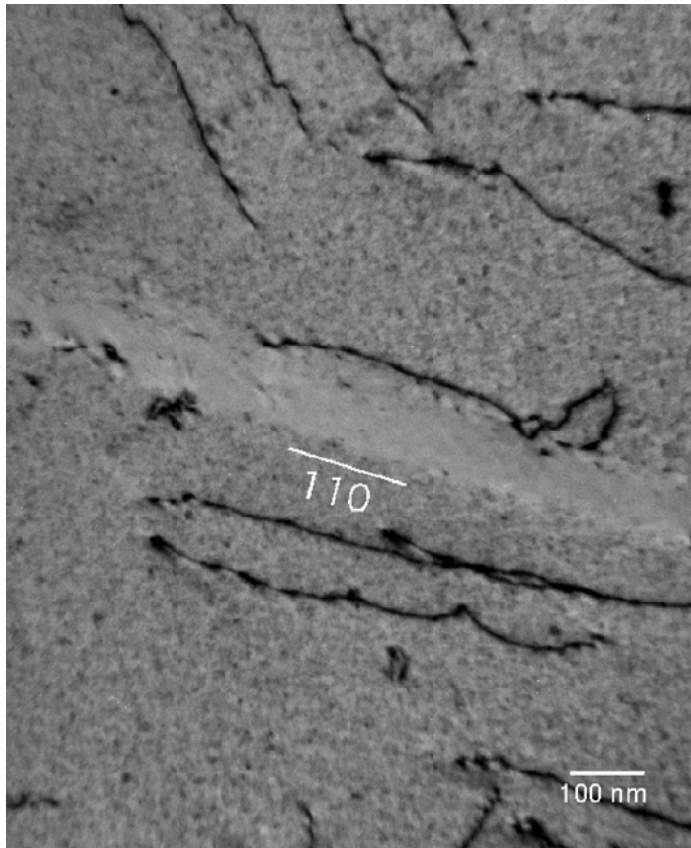
## Copper

$3.5 \times 10^{-2}$  dpa  
 $\gamma = 15 \%$

# Dislocation channel in Fe12Cr



**Defect-free channel** in deformed proton-irradiated Fe-12Cr alloy at room temperature to 0.2 dpa.  
Imaging conditions: BF,  $g = \{110\}$ ,  $ZA = \langle 111 \rangle$ .



# Channel Characteristics

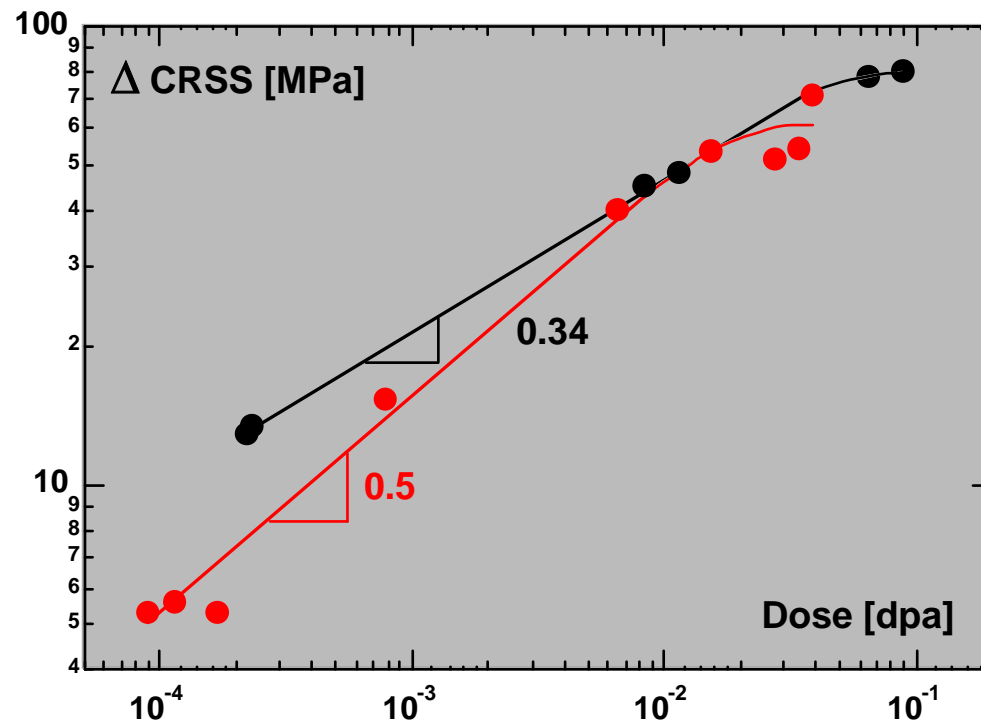
- Channels on  $\{111\}$  planes in fcc and  $\{110\}$  (sometimes  $\{112\}$ ) in bcc.
- Interchannel density of defects or density near channel walls is the same as in the as-irradiated crystal: no displacement of defects from the channel by moving dislocations.
- Channel thickness in Cu/Pd: 100-200 nm
- Channel separation (parallel channels):  $1\mu\text{ m}$

# Channel Characteristics

- From measurements of the offset on one channel produced by another channel (in Pd):
  - 450 slip planes per channel
  - offset per slip plane: 209 nm or 2 dislocations per slip plane. from other observations in Cu/Nb: 1-3 dislocations per slip plane.
- Taking the measured value of the defect size (2 nm), there are 10 slip planes per defect.
- Total shear strain associated with a channel: 0.5-0.7

# Change in CRSS versus Dose

different behavior for Pd and Cu



## Radiation hardening (I)

### Source hardening

- Taking for Cu ( $\mu = 55$  GPa,  $b = 0.256$  nm) the value of  $\tau_{UY} = 50$  MPa measured in a Cu crystal irradiated with protons to  $6.6 \cdot 10^{-3}$  dpa, the relation

$$ly^2 = 118 \text{ nm}^3$$

is obtained when the measured average value of  $d = 2.05$  nm is used.

- The stand-off distance  $y$  is unknown and atomistic calculations are needed to get its proper value, but it can be estimated to be of the order of the loop size  $d$ . The distance  $l$  must then be of the order of  $10b$  (3.6 nm) in order to account for the upper yield point, which compares well with that of TEM observations.

## Radiation hardening (II)

### Dispersion hardening

- There is in addition a distribution of loops in the rest of the crystal matrix, at a lower density and larger spacing than those locking the original dislocations.
- The unlocked source dislocation will glide and interact with the distribution of defect clusters present in the matrix of the crystal.
- Defect cluster mean distances: for Cu at  $6.6 \cdot 10^{-3}$  dpa, the mean distance in the matrix is  $L = (Nd)^{-1/2} \cdot 280$  nm, a factor of about one hundred times larger than the value for dislocation locking.

## Radiation hardening (II)

### Dispersion hardening

- The hardening by this defect structure is well represented by the dispersed obstacle model, where the increase of strength, beyond the upper yield point, compared to the unirradiated state, is given by:

$$\Delta\tau = \alpha\mu b (Nd)^{1/2}$$

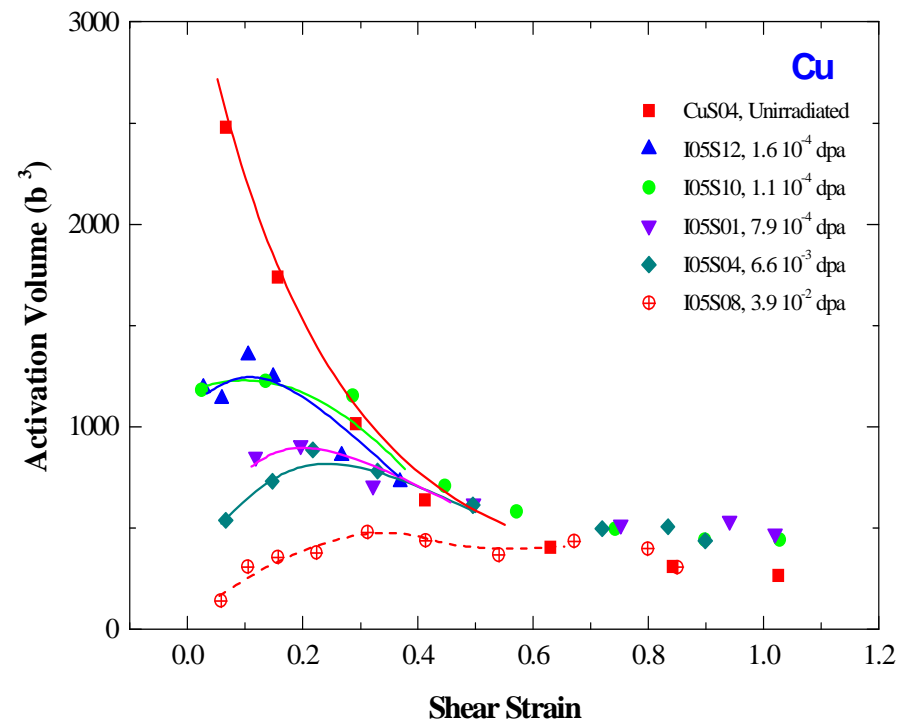
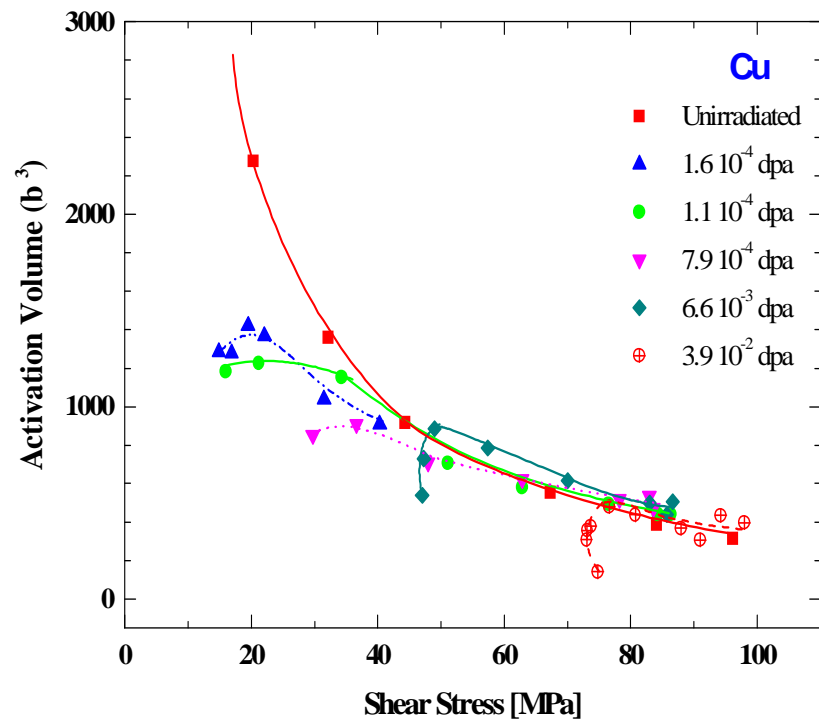
$\alpha$  is a factor that accounts for the strength of the obstacle.

## Radiation hardening (II)

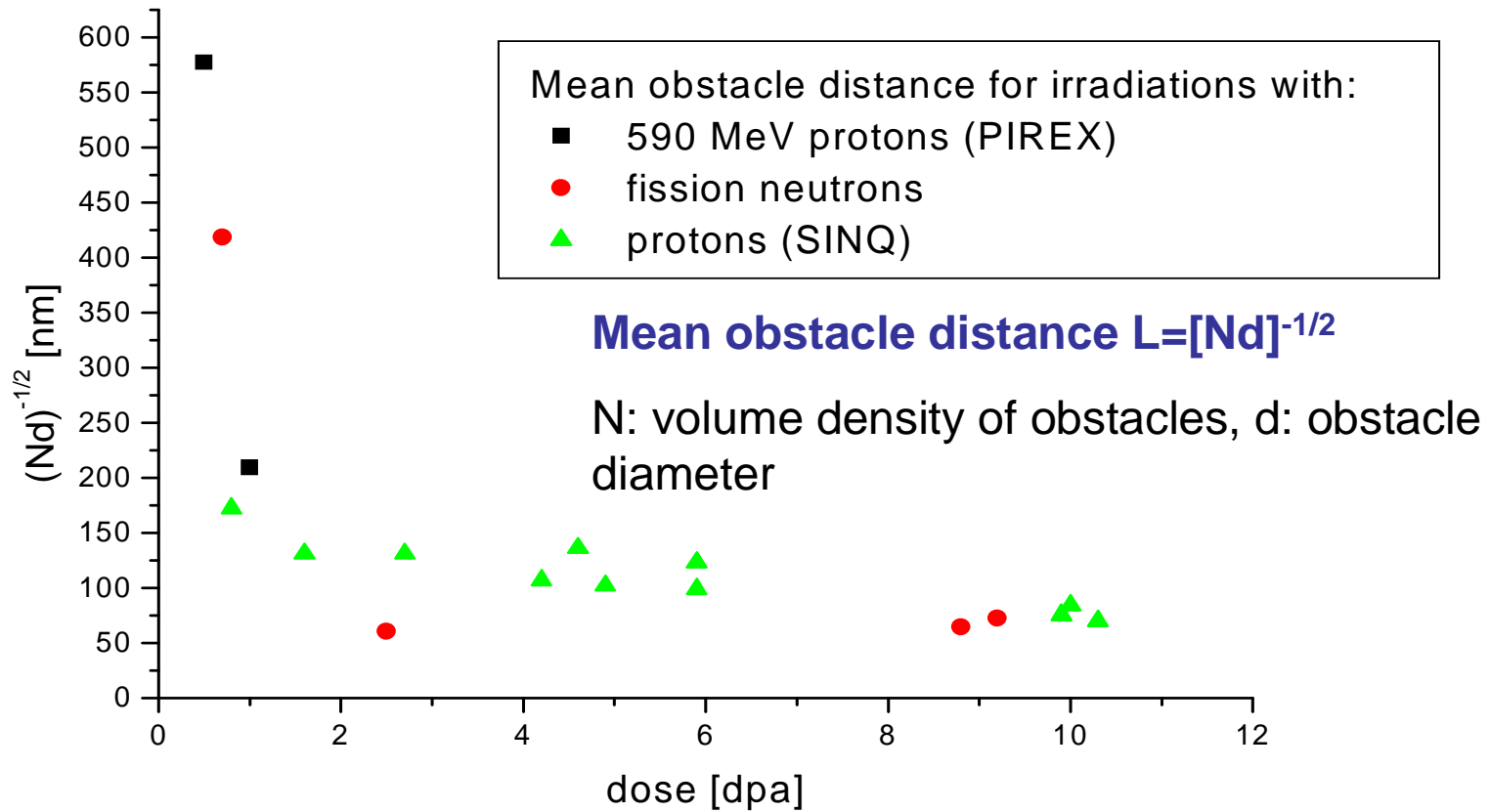
### Dispersion hardening

- In the irradiated Cu and Pd single crystals there is a linear relation between the measured values of  $\Delta\tau$  and  $(Nd)^{1/2}$  with a resultant value of  $\alpha = 0.1-0.2$ , which describes soft obstacles.
- Beyond the yield region, the contribution from dislocation-dislocation interaction to the work hardening is the main component of the flow stress.

# Activation volumes in irradiated Cu



# The obstacle mean distance controls the hardening



# Dispersed Obstacle Hardening Model

Bement 1970; Kojima, Zinkle and Heinisch 1991

$$\Delta \text{CRSS} = \alpha \mu b \sqrt{\rho d}$$

$$\alpha = 0.9 \left\{ \cos \left( \phi/2 \right) \right\}^{3/2}$$

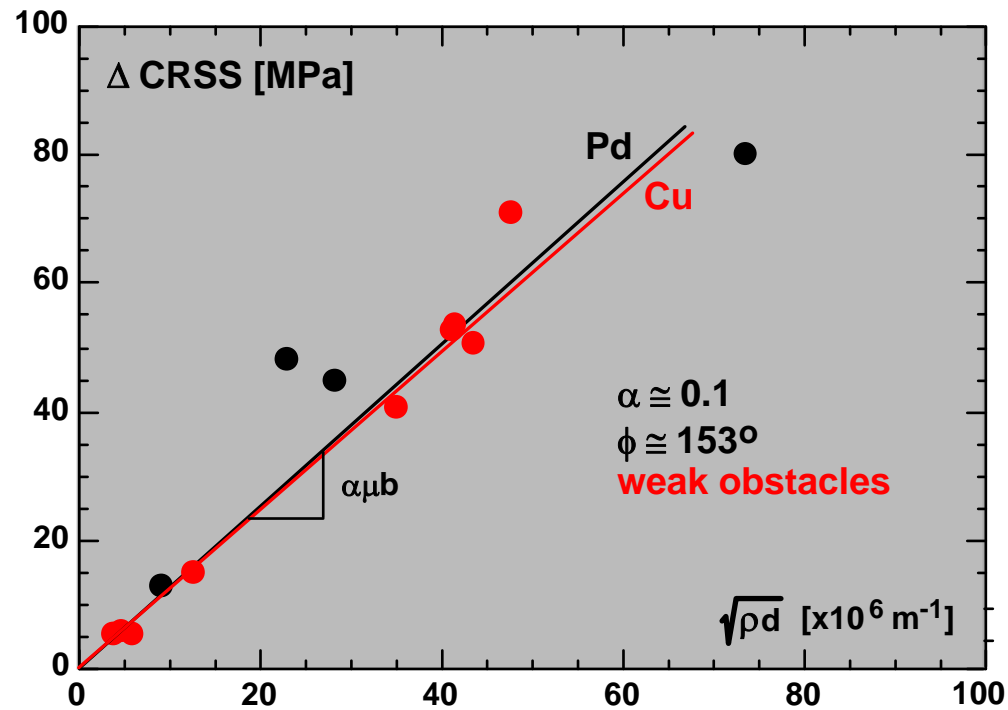
$\alpha$  = constant related to the strength of defect clusters

$\mu$  = shear modulus

$b$  = magnitude of  $\langle 110 \rangle$  Burgers vectors

$\rho$  = defect cluster density

$d$  = mean defect diameter



# A multiscale model for the behavior of irradiated pure fcc metal single crystals

- The recoil energy spectra corresponding to the beam used in the irradiation is calculated.
- A library of cascades produced by recoils of energies typical of this distribution is constructed. The information noted is that of the resulting number of single defects and clusters as well as their types
- This information is fed to an object kMC code together with other information, such as the different reactions between single defects and clusters
- Information on the number of cluster of an **observable size (>1 nm)** as a function of dose is extracted

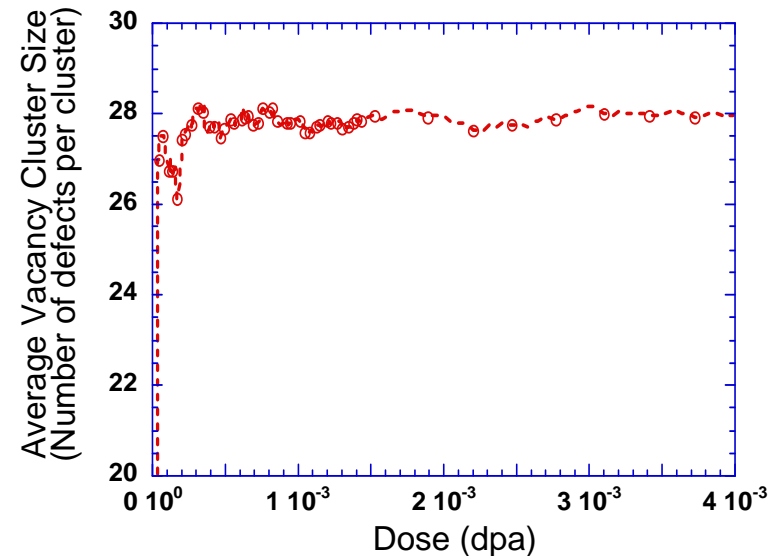
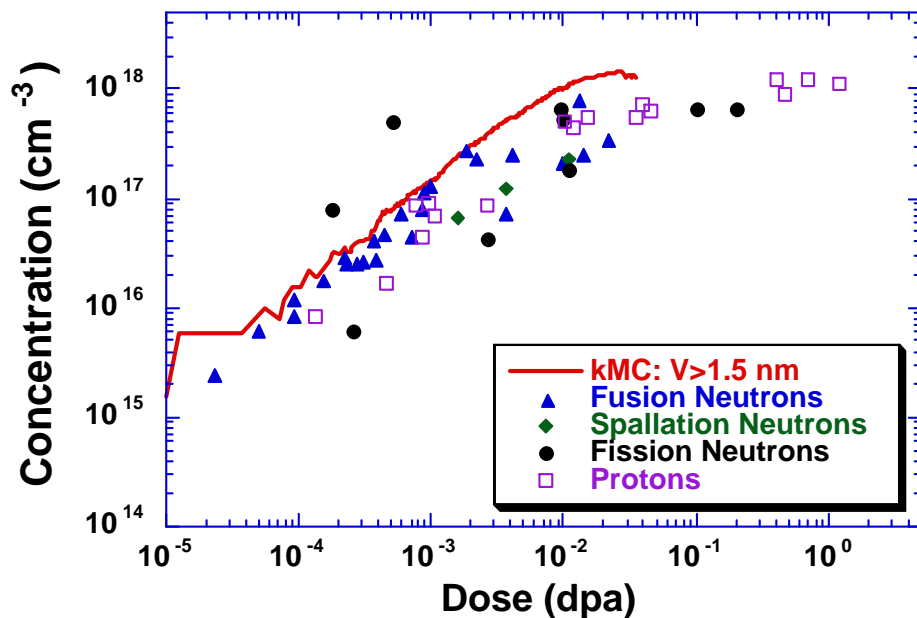
Diaz de la Rubia, Zbib, Khraishi, Wirth, Max Victoria and Caturla;  
Nature **406** (2000) 871

# Validation of multiscale modeling of defects produced by cascades: comparison to experimental measurements (LLNL)



Defect concentration in Copper irradiated with Neutrons and Protons compared to kMC simulations

Damage Accumulation in Copper



- The average size of Vacancy clusters is constant with dose in agreement with experiments. Cluster size ~ 1.7 nm.
- Experimental values are ~ 2 nm average cluster size.

# Dislocation dynamics simulation

- The time evolution of the motion and interaction of an ensemble of dislocations is followed in a  $5\mu\text{m}^3$  cube of material. It initially contains a density of Frank-Read sources randomly distributed in  $\{111\}$  planes.
- Dislocations are discretized into straight line segments of mixed character.
- To ensure continuity of dislocation lines across the boundaries, reflection boundary conditions are used.

# Dislocation dynamics simulation

- The Peach-Koehler force  $F$  acting on a dislocation segment is calculated from the stress fields of (a) neighboring segments, (b) all other dislocation segments, (c) all defect clusters and (d) the applied stress.
- The result is used to advance the dislocation segment based on linear mobility  $v_{gi} = M_{gi}F_{gi}$  ( $M_{gi}$ : dislocation mobility,  $F_{gi}$ : glide component of Peach-Koehler force minus the Peierls friction).
- Segments about to experience short range interactions are identified. Reactions might result in formation of junctions, jogs, dipoles.

# Dislocation dynamics simulation

- Cross-slip is described as an activated process with probability  $P$  given by:

$$P = \alpha \Omega_l \delta t \exp [-(\Omega - \tau A)/kT] \quad \text{for} \quad \Omega_l = C_t \pi / L$$

- Defects (SFT's or Frank sessile interstitial loops) are mapped into the DD box in densities in accord to those produced by a particular fluence and temperature.
- Decorated F-R sources are also introduced.
- Detailed atomistic modeling of the dislocation-defect interaction are performed in MD simulations

# Dislocation-SFT interaction (From B. Wirth)

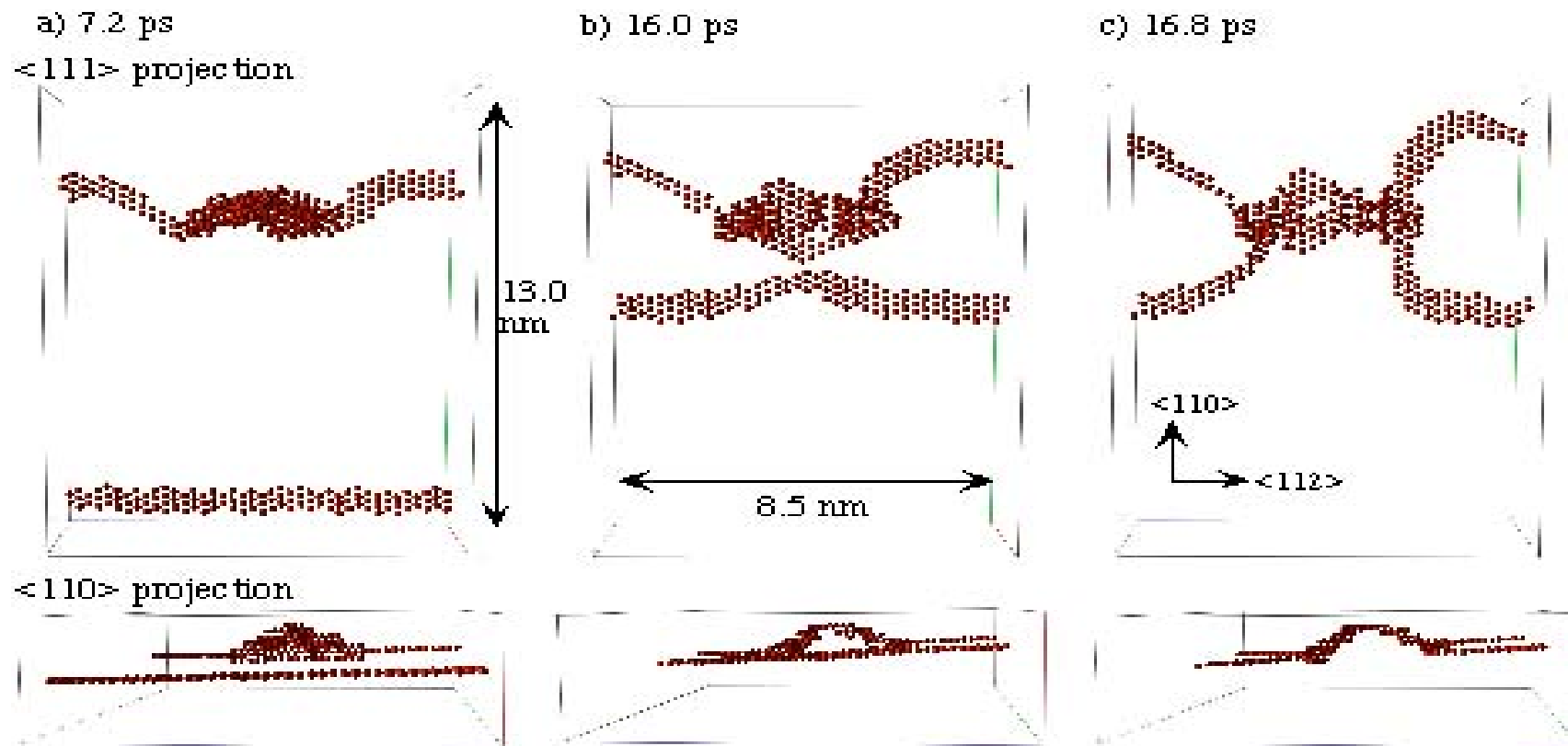
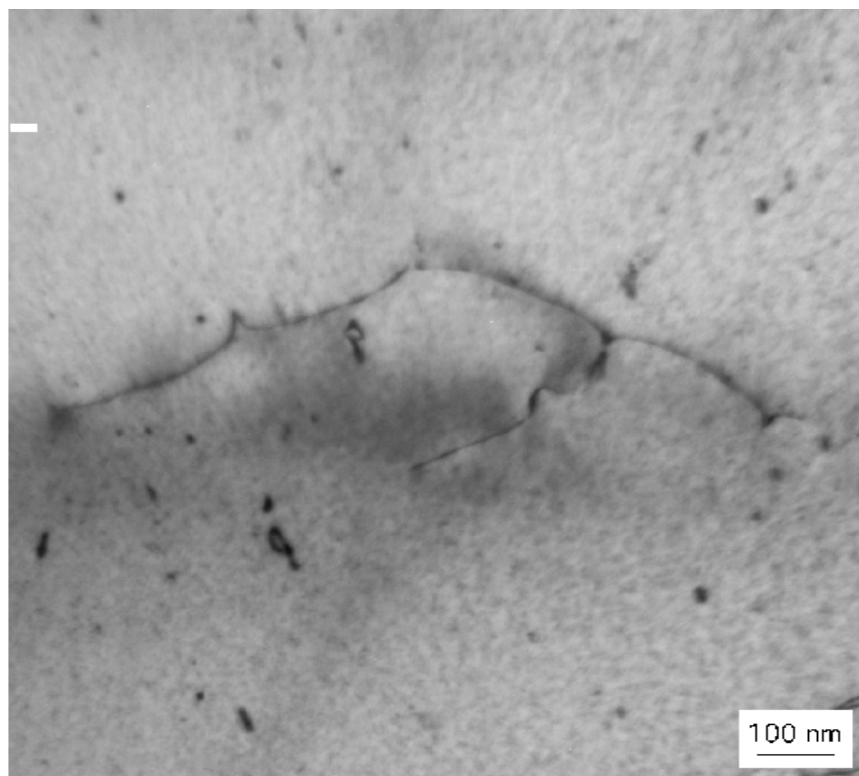
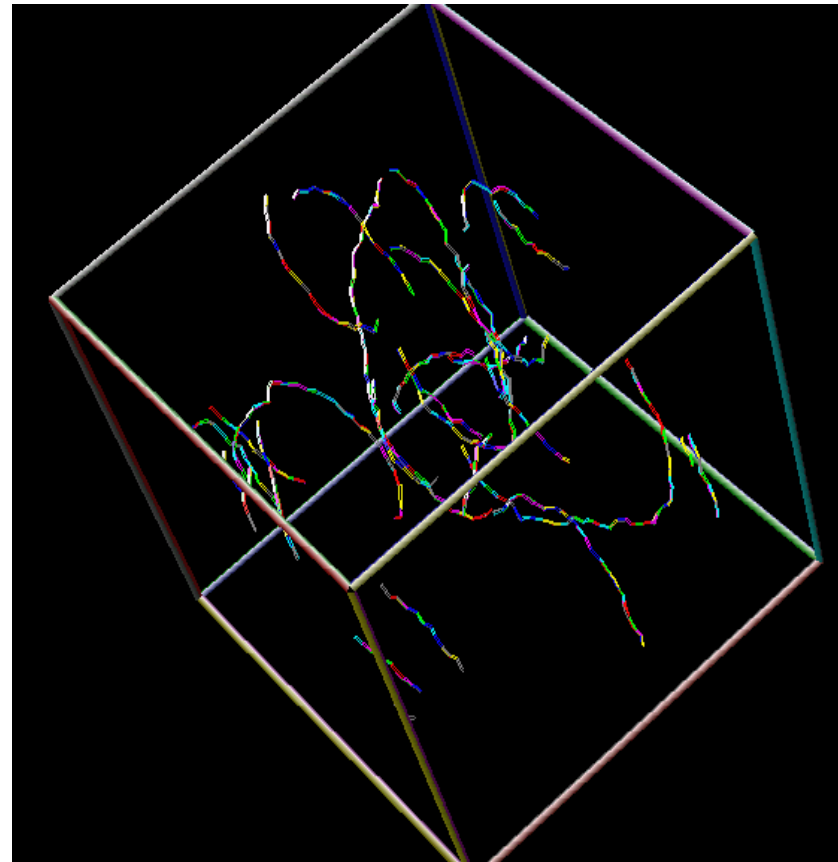
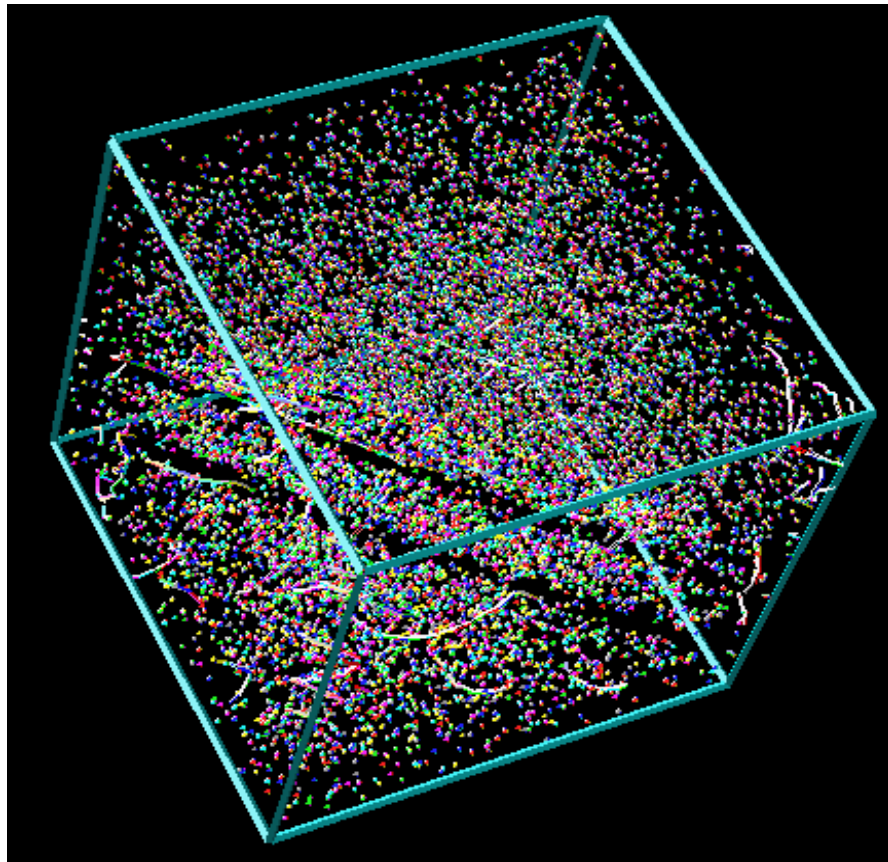


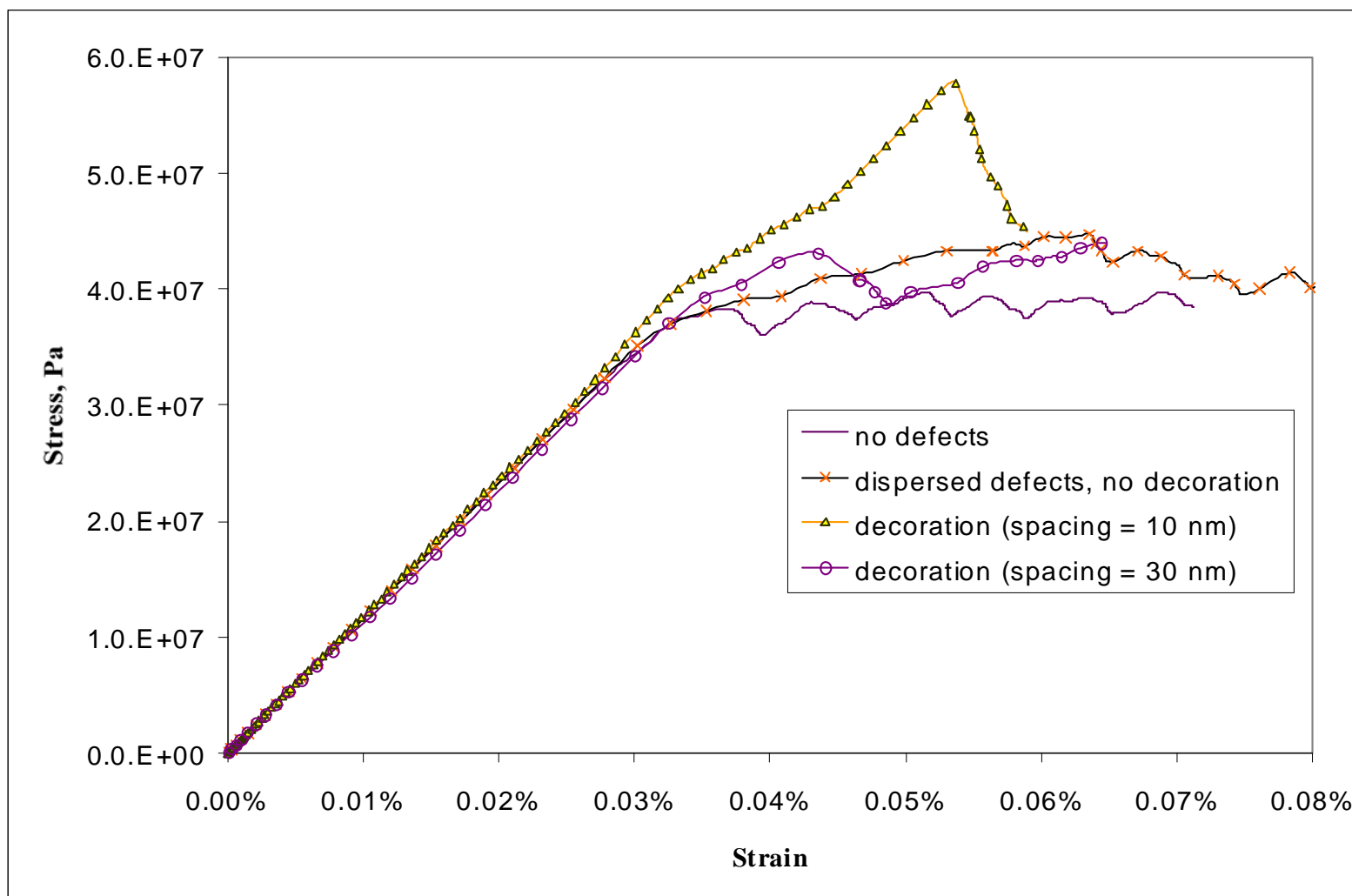
Figure 2 --  $\langle 111 \rangle$  (top) and  $\langle 110 \rangle$  (bottom) projections of high energy atoms showing the motion of two Shockley partials on their  $\{111\}$  glide plane and interaction with an overlapping SFT at a) 7.2, b) 16.0 and c) 16.8 ps after application of a shear stress.



# The interaction of dislocations with SFT's

In situ TEM observations in irradiated Cu  
(Yao and Schaublin)





# Summary

The results of irradiations in fcc Cu, Pd and 304L austenitic stainless steel and with either fission neutrons or 590 MeV protons indicate that:

- A high density ( $10^{22}$ - $10^{24}$  m<sup>-3</sup>) of defect clusters is found. The majority of clusters are SFT's in Cu while in Pd and Fe they are interstitial loops, showing that for low stacking fault energy metals (Cu), SFT's form, while loops are the main component of the microstructure for high SFE metals Pd and Fe. Austenitic stainless steels are an exception to this trend in that the SFE is low but loops are formed.